Université Mohamed Khider de Biskra
Faculté des sciences Exactes des Sciences de la Nature et de la Vie
Département des Sciences de la matière

MÉMOIRE DE MASTER

Domaine de Science de la matière
Filière de Chimie
Chimie des matériaux

Réf. :

Présenté et soutenu par :
Bacha Nour El Houda

Le : 18/06/2023

Theoretical study on the effect of corrosion inhibitors of a plant extract

---

Jury :

Mr	Kenouche Samir	MCA	Université Mohamed Biskra	Président
Mr	Sellami Mohamed	MCB	Université Mohamed Biskra	Encadrant
Mr	Chadli Abd El Hakim	MCA	Université Mohamed Biskra	Examinateur

Année universitaire : **2022/2023**

Acknowledgements

I would like to express my warm thanks to my supervisor Dr. Mohamed Sellami, Department of Matter Sciences, for his entire disposition, and judicious advice, and for having directed me throughout my project work. I would like to express my deepest appreciation to Dr.Salah Hachani for the time, effort, and invaluable advice that went into the process. I especially appreciate the feedback provided.

I would also like to thank Dr. S Kenouche and Dr. A Chadli, Department of Matter Sciences, for having accepted to be part of the jury of this work as examiners.

My thanks and gratitude to our teachers who throughout the years of study have passed on their knowledge to us.

My thanks also go to all who have contributed directly or indirectly to the development of this work.

Finally, I would also express my deep sense of gratitude to my family members and my friends for their encouragement and support throughout, which always inspired me.

Dedicate

This modest work is dedicated to:

My parents

Whom affection, love, encouragement, and prayer of day and night make me able to get such success and honor,

My brothers Oussama and his wife Widad ,Mosaab and Yocef also my sisters Soumya , Afaf, Aicha,oumaima.

My friends Maryem and Safa ,Ikram, Samah, Sirin , Aya, Maroua, Roumaissa as a constant source of support and encouragement during the challenges of graduation,

All my friends and my family.

Abbreviations list

VCIs: volatile corrosion inhibitors

GA: Ancymidol Gibberellins

SEM: scanning electron microscopy

GTE: green tea extract

CS: C38 Steel

BTE: black tea extract

LSCM: laser scanning confocal

CP: Carrot peels

DCA: Daucus Carota aerial

DFT: density functional theory

LDA: Local density approximation

LSDA: Local Spin Density Approximation

GGA: Generalized Gradient Approximation

NLD: Non-Local Density

SAR: structure-activity relationship

B3LYP: Becke 3 Lee Yang Parr exchange

SCRF: a self-consistent reaction field

HOMO: Highest Occupied Molecular Orbital

LUMO: lowest unoccupied molecular orbital

List of figures

Chapter I: Generalities about the corrosion phenomenon

Chapter III: Analyzing organic compounds reactivity using DFT

List of tables

Chapter I: Generalities about the corrosion phenomenon

Chapter III: Analyzing organic compounds reactivity using DFT

Abstract

DFT-derived global reactivity descriptors, Mulliken charges, and SAR parameters have been calculated in aqueous phase at DFT/B3LYP/6-31G theoretical level to bridge the gap between the effect of electronic properties at the molecular level and the inhibition efficiency of mild steel corrosion in an acidic medium using two molecules namely ([(2R,3R)-5,7-dihydroxy-2-(3,4,5-trihydroxyphenyl)-3,4-dihydro-2H-chromen-3-yl]3,4,5-trihydroxybenzoate) (COMP1) and ((1S,3R,4R,5R)-3-[(E)-3-(3,4-dihydroxyphenyl)prop-2-enoyl]oxy-1,4,5 trihydroxycyclohexane-1-carboxylic acid) (COMP2). The obtained results of the global reactivity descriptors as well as SAR parameters show some positive agreement with the experimental outcomes of the corrosion inhibition efficacies. Mulliken charge analysis gives a comprehensive view of the atoms responsible for the electron transfer from the studied inhibitor molecules to the mild steel surface to prevent the corrosion phenomenon.

Keywords: DFT-global reactivity descriptors, SAR, Mulliken charge, COMP1, COMP2, corrosion inhibitors.

RÉSUMÉ

Les descripteurs de réactivité globale dérivés de DFT, les charges Mulliken et les paramètres SAR ont été calculés en phase aqueuse au niveau théorique DFT/B3LYP/6-31G pour combler l'écart entre l'effet des propriétés électroniques au niveau moléculaire et l'efficacité d'inhibition de l'acier doux corrosion en milieu acide à l'aide de deux molécules à savoir ([(2R,3R)-5,7-dihydroxy-2-(3,4,5-trihydroxyphenyl)-3,4-dihydro-2H-chromen-3-yl]3 ,4,5-trihydroxybenzoate) (COMP1) et ((1S,3R,4R,5R)-3-[(E)-3-(3,4-dihydroxyphényl)prop-2-énoyl]oxy-1,4, acide 5-trihydroxycyclohexane-1-carboxylique) (COMP2). Les résultats obtenus des descripteurs de réactivité globale ainsi que des paramètres SAR montrent un certain accord positif avec les résultats expérimentaux des efficacités d'inhibition de la corrosion. L'analyse de charge Mulliken donne une vue complète des atomes responsables du transfert d'électrons des molécules d'inhibiteur étudiées vers la surface de l'acier doux pour empêcher le phénomène de corrosion.

Mots clés : DFT-descripteurs de réactivité globale, SAR, charge de Mulliken, COMP1, COMP2, inhibiteurs de corrosion.

ملخص

تم حساب مؤشرات التفاعل الكلية المشتقة من DFT ، وشحنات Mulliken ، ومعلمات SAR في الوسط المائي عند المستوى النظري DFT / B3LYP / 6-31G لتحديد تأثير الخصائص الإلكترونية على المستوى الجزيئي وكفاءة تثبيط الفولاذ الطري التآكل في وسط حمضي باستخدام جزيئين هما ()R2[، 5- (3،3R) -2-dihydroxy-4،7،5- (trihydroxyphenyl) -3 ، 3 [4-dihydro-2H-chromen-3-yl ، 4،5-ثلاثي هيدروكسي بنزوات) (COMP1) و

(1S ،3R ،4R ،3- (5R - [3- (E)- (3،4)-ثنائي هيدروكسي فينيل) prop-2-enoyl] أوكسي-1،4 ، 5 ثلاثي هيدروكسي سيكلوهكسان -1 حمض كربوكسيل) (COMP2). أظهرت النتائج المتحصل عليها من مؤشرات التفاعل الكلية وكذلك معاملات SAR بعض التوافق الإيجابي مع النتائج التجريبية لكفاءة تثبيط التآكل. يعطي تحليل شحنة Mulliken نظرة شاملة للذرات المسؤولة عن نقل الإلكترون من جزيئات المثبط المدروسة إلى سطح الفولاذ الطري لمنع ظاهرة التآكل.
الكلمات المفتاحية: مؤشرات التفاعل الكلية DFT، SAR، شحنة Mulliken، COMP1، COMP2. مثبطات التآكل

General introduction

General introduction

Mild steel is an excellent engineering material widely used for its excellent malleability and high mechanical strength in several industrial applications such as chemical storage and transportation. Mild steel can be easily corroded under the effect of various aggressive media, which leads to altering its physical properties, and therefore reducing its industrial performance [1].

The use of corrosion inhibitors has become a reliable method used to protect mild steel against corrosive agents. Heterocyclic molecules containing polar functional groups and conjugated double bonds are expected to be effective mild steel corrosion inhibitors. The inhibitory performance of these chemical compounds is attributed to their adhesion to the metal surface via either physical adsorption through electrostatic interactions between an opposing charged metal surface and the corrosion inhibitor, or chemical adsorption using electron coordination bonds of the lone pair of heteroatoms (O, S, N, and P) or a lone ring in the structure of the corrosion inhibitor with a metallic surface [2].

Mechanisms of corrosion inhibition can be studied using chemical and analytical techniques such as electrochemical measurements and weight loss tests. These experimental techniques are costly and time-consuming, and in some cases, they are not sufficient to explain the observed phenomena [3].

The gigantic revolution in the field of computing facilitates the analysis and interpretation of all physical and chemical properties using theoretical quantum calculations based on many theories such as density functional theory DFT which has become a reliable tool widely used to provide valuable explanations of inhibition mechanisms. Theoretical studies of gas-phase and water-phase corrosion inhibitors have shown that the corrosion-inhibiting effectiveness of an inhibitor is closely related to quantum chemical descriptors such as the energy of the highest occupied molecular orbital E_{HOMO} and energy of lowest unoccupied molecular orbital E_{LUMO}, electronegativity, hardness, softness and fraction of electron transferred. In fact, the above stand-alone molecular properties cannot provide a realistic model for the interactions of the inhibitor with the metal surface. Molecular dynamics (MD) simulations are then considered because of their ability to reproduce the real interactions of the inhibitor with the metal surface and to describe well the structural configuration of the inhibitor in the corrosion process [4].

In recent studies, epigallocatechin gallate ([(2R,3R)-5,7-dihydroxy-2-(3,4,5-trihydroxyphenyl)-3,4-dihydro-2H-chromen-3-yl]3,4,5-trihydroxybenzoate) (COMP1) and chlorogenic acid ((1S,3R,4R,5R)-3-[(E)-3-(3,4-dihydroxyphenyl)prop-2-enoyl]oxy-1,4,5 trihydroxycyclohexane-1-carboxylic acid) (COMP2) were extracted and their inhibitory role on the corrosion of mild steel in a HCl medium of 1.0 M concentration was investigated. These molecules have been found to be excellent corrosion inhibitors and the experimental order of inhibition rate is as follows: COMP2 > COMP1

As far as, no theoretical study has been proposed yet to correlate the experimental efficiency of the previous corrosion inhibitors and their electronic features at molecular scale. DFT and SAR approaches have been used to give different descriptors to be correlated with the experimental data earlier reported.

This manuscript comprises three key chapters that collectively contribute to our understanding of corrosion and the development of green corrosion inhibitors:

- Chapter I serves as an introduction, providing a comprehensive overview of corrosion, including its various forms and classification. This chapter also offers a broad perspective on the current state of research concerning the study of plant extracts as eco-friendly corrosion inhibitors. By delving into the fundamental concepts and key findings in this field, Chapter I sets the stage for the subsequent chapters.
- Chapter II focuses on presenting the density functional theory (DFT) as a potent quantum tool for investigating corrosion phenomena. In this chapter, the application of DFT is explored, with particular emphasis on its hybrid functionals and basis sets. Moreover, a concise yet comprehensive description of global and local reactivity parameters is provided, enabling a deeper understanding of the reactivity patterns of corrosion processes.
- Chapter III builds upon the foundation laid in the previous chapters by elucidating the diverse outcomes of global reactivity descriptors, Mulliken charge analysis, and structure-activity relationship (SAR) investigations. By delving into these findings, the chapter facilitates a deeper understanding of the electronic characteristics of the studied molecular systems and their influence on inhibitory performance. Through insightful discussions and analysis, Chapter III effectively bridges the gap between molecular properties and their impact on corrosion inhibition.

References

[1] K. Adel, S. E. Hachani, I. Selatnia, N. Nebbache, and S. Makhloufi, 'Correlating the inhibitory action of novel benzimidazole derivatives on mild steel corrosion with DFT-based reactivity descriptors and MD simulations', *J. Indian Chem. Soc.*, vol. 99, no. 7, p. 100497, 2022.

[2] R. Baskar, H. Lgaz, and R. Salghi, 'Heterocyclic Compounds as Corrosion Inhibitors for Mild Steel: A Review', *Chem. Sci. Eng. Res.*, vol. 1, no. 1, Aug. 2019, doi: 10.36686/Ariviyal.CSER.2019.01.01.005.

[3] I. Obot, D. Macdonald, and Z. Gasem, 'Density functional theory (DFT) as a powerful tool for designing new organic corrosion inhibitors. Part 1: an overview', *Corros. Sci.*, vol. 99, pp. 1–30, 2015.

[4] G.-J. Cheng, X. Zhang, L. W. Chung, L. Xu, and Y.-D. Wu, 'Computational Organic Chemistry: Bridging Theory and Experiment in Establishing the Mechanisms of Chemical Reactions', *J. Am. Chem. Soc.*, vol. 137, no. 5, pp. 1706–1725, Feb. 2015, doi: 10.1021/ja5112749.

Chapter 1

Generalities about the corrosion phenomenon

This first chapter focuses on a theoretical study on corrosion, these differents categories as well as the various types of corrosion protection, especially green inhibitors. Also, a general averveiw of the present state of research on the study of plant extracts as corrosion inhibitors on metal surfaces in corrosive media was presented.

I.1. Corrosion process

In simple terms, corrosion can be described for the purposes of this chapter as the degradation of a metal or its qualities as a result of its reaction with its environment, which includes the complete surrounding in touch with the substance [1]. This process caused by chemical or electrochemical reactions with its environment. In general, it involves the loss of metal due to oxidation or reduction reactions. Typically, once a metal corrodes, it forms compounds known as oxides or hydrated oxides.

Figure I. 1: *corroded hinge [2].*

I.1.1. Factors affecting corrosion rate

The phenomena of corrosion depend on a large number of factors and they can be classified into four main groups as the table shows (Table I.1) [3].

Tableau I. 1: *Factors affecting corrosion rate.*

Corrosive environmental factors	**Metallurgical factors**	**Factors defining conditions of employment**	**Time dependent Factors**
- Reagent concentration - Oxygen content - pH of the medium - Temperature - pressure	- Composition of the alloy -Development processes - Impurities - Heat treatment -Mechanical treatment	- Surface condition - Shape of parts - Use of inhibitor -Assembly processes	- Aging - Mechanical tensions - Modification of protective coatings

I.1.2. Different forms of corrosion

Understanding the different types of corrosion is important in developing effective strategies to prevent and mitigate their effects on metallic materials.

The various types of corrosion can be divided into two categories: general and localized corrosion. This type includes many modes of corrosion (crevice or underdeposit corrosion, galvanic corrosion, erosion corrosion, fretting corrosion, corrosion fatigue, etc.).

I.1.2.1. General corrosion

General corrosion is the most common form of corrosion, also known as uniform corrosion. It is distinguished by an electrochemical or chemical reaction that occurs on the exposed surface. When the metal gets thinner, it finally fails and perforates. On a tonnage basis, general corrosion is responsible for the majority of metal loss [1]. for example rusting of steels in oping air.

I.1.2.2.Localized corrosion

One of the largest isuues for material selection for application is localised corrosion, it comes with different modes like galvanic,crevice ,Pitting corrosion…[4]. As simply as its name, localized corrosion is a form of corrosion that occurs in specific areas of a material's surface. This process often begins with the formation of small pits or depressions on the surface (deep and fast penetration), which can expand over time and weaken the material [5].

a) Galvanic corrosion

When two metals or alloys with different nobilities and, consequently, different electrochemical potentials come into contact with one another under water or in a damp environment, galvanic corrosion results. In this situation, the less noble metal serves as an anode, and the more noble metal serves as a cathode (figure I.2). It is always for anode that corrodes [6].

ssThe rate of galvanic corrosion is affected by several factors,wich indicates how much material (often measured in thickness or weight) is lost to corrosion over time taking into account [7]. The difference in the nobility of the metals, the surface area of the metals in contact, the conductivity of the electrolyte, the temperature and pH of the environment [8].

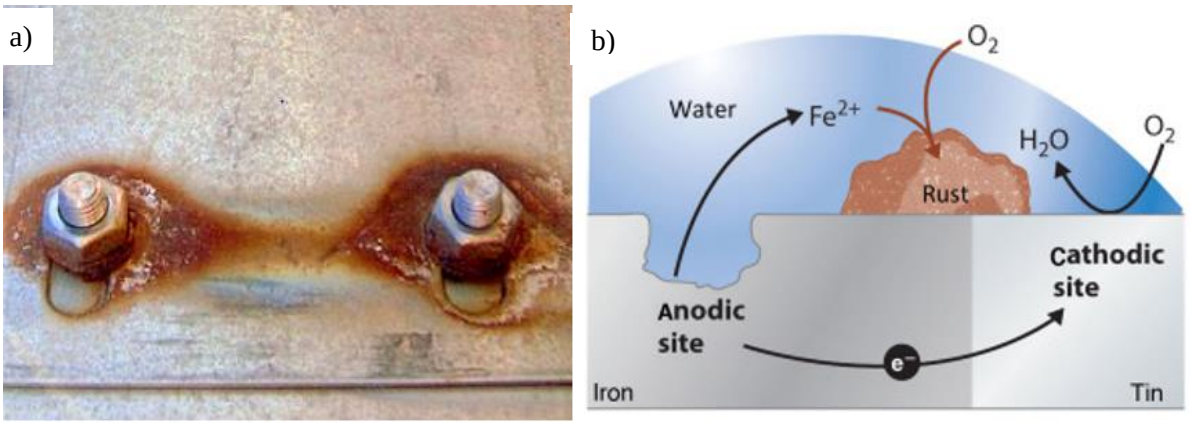

Figure I. 2: *a) stainless steel –mild steel cropped, b) mechanism o the galvanic corrosion [9].*

b) Crevice corrosion

In occluded areas or crevices of metallic components, crevice corrosion is a type of limited assault,this phenomenon is brought on by regional variations in the electrolyte's ion concentration and because of that, there was a potential diffrence [10].

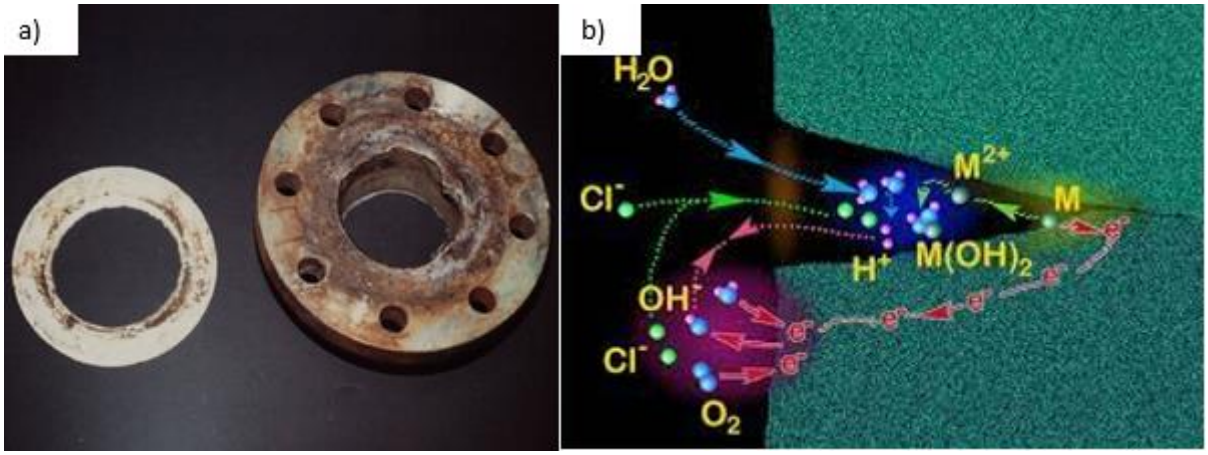

Figure I. 3: *(a)Typical View of Crevice Corrosion [11].and (b)its mechanism[12].*

c) Pitting corrosion

It affects the outer surface by creating holes and becomes anodic, that quickly and significantly grow. alloys that rely on an oxide coating for protection, such as stainless steel, are prone to pitting [13]. The following figure shows the mechanism of pitting corrosion.

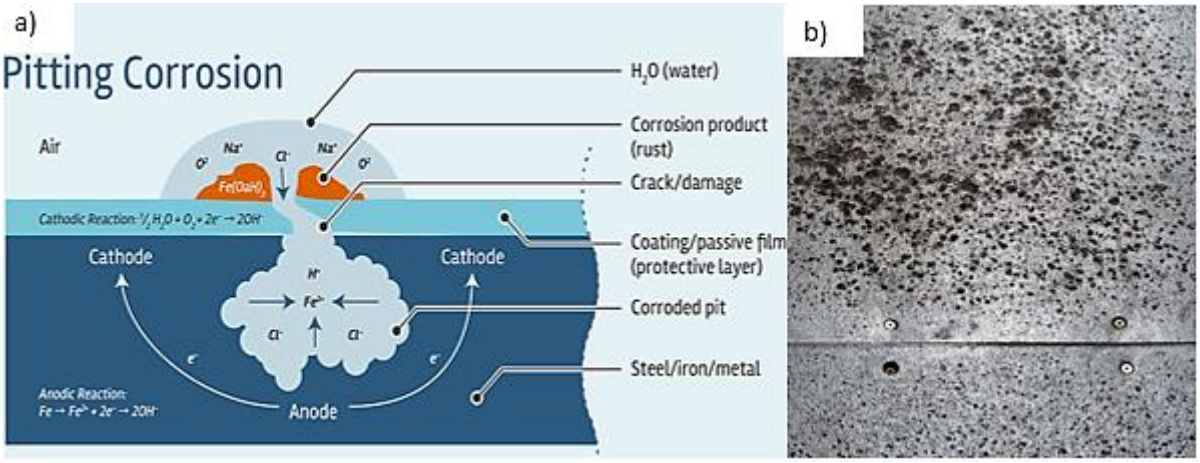

Figure I. 4: ***(a)*** *Pitting corrosion diagram [14].****(b)*** *holes due to pitting corrosion[15].*

d) Dealloying or selective leaching

It is the process by which one solid element is eliminated from alloy by corrosion. this phenomenon can be obviously distinguished in the dezincification of brass (figure I.5), in which zinc selectively defects from a copper–zinc brass alloy [16].

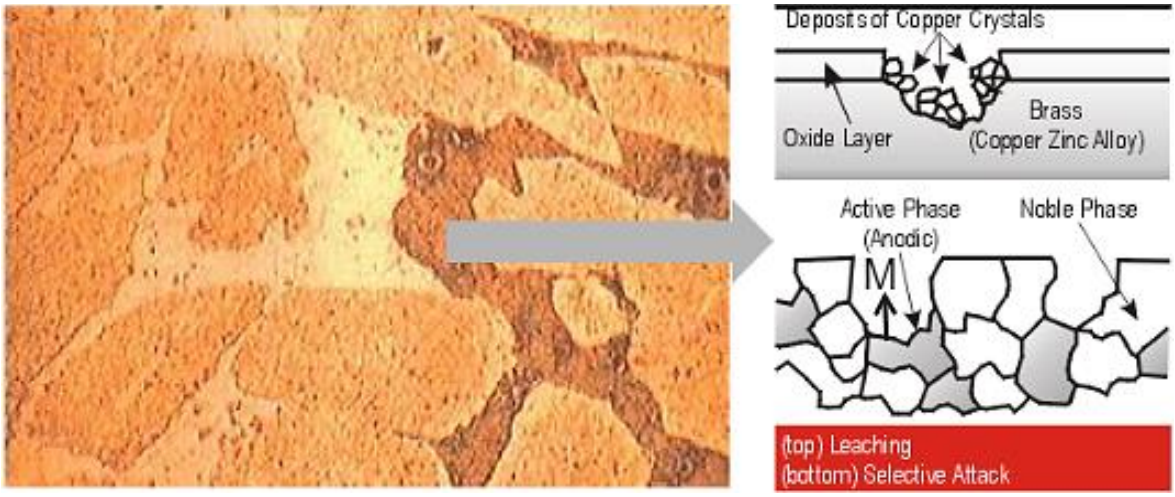

Figure I. 5: *Mechanism of selective corrosion of a brass (copper-zinc alloy).*

e) Intergrannular corrosion

In materials science, the grain and grain boundaries of metals and their alloys lead to different mechanical properties. In certain environments, the presence of impurities such as acids, salts, the presence of carbides in alloys or other factors can attack the grain boundaries which affects in-depth along the grain boundaries, which leads to a micro-crack, then the surface does not show any alteration [1].

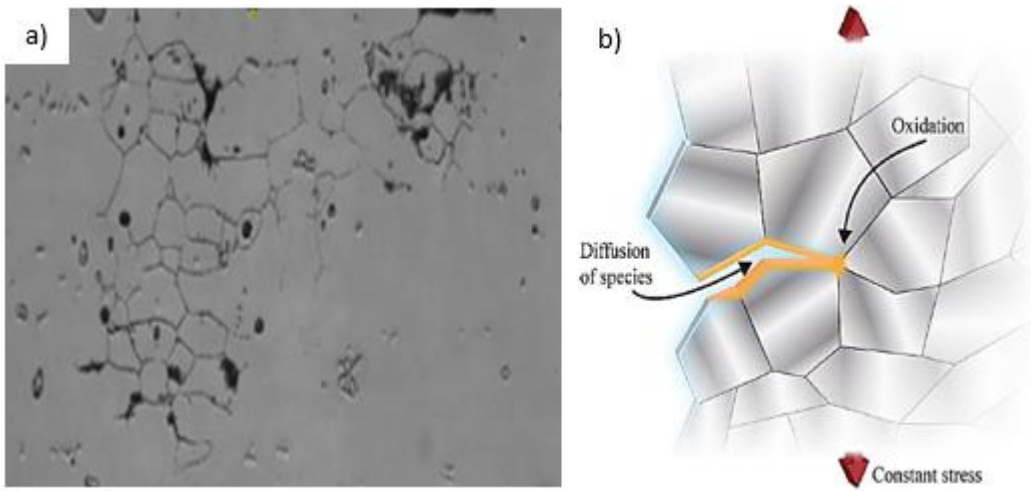

Figure I. 6: *(a) Intergrannular attack in aluminum alloy [17] and (b) Schematic figure of material undergoing constant stress [18].*

f) Erosion Corrosion

This type of corrosion is known as impingement or water drop corrosion. On another hand, erosion-corrosion is the process by which the attack on a metal is accelerated or increased as a result of changes in the velocities of corrosive fluids and metal surfaces.

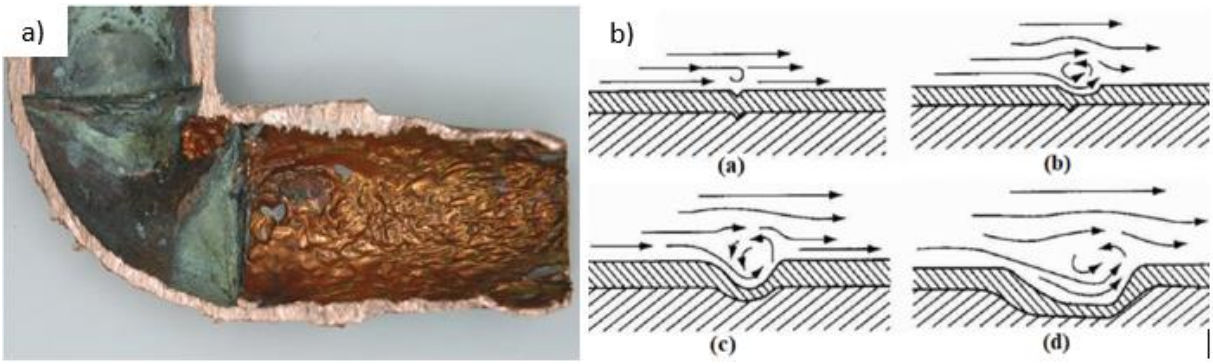

Figure I. 7: *(a) Erosion-corrosion in a section of piping[19], (b) Erosion-corrosion stages [20]*

g) Fretting corrosion

Fretting corrosion is the deterioration of the material which occurs at the interface of two surfaces in contact due to small oscillating movements which occur between them in the presence of a corrosive environment [21].

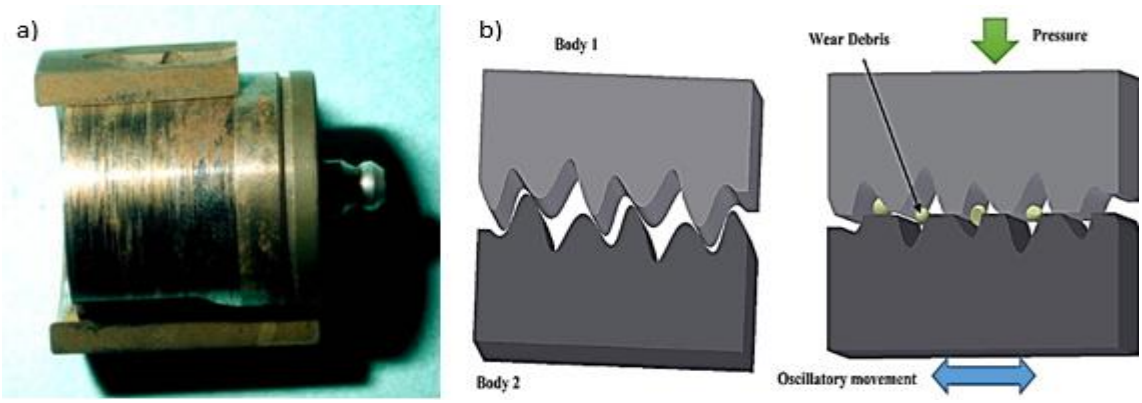

Figure I. 8: *(a) Fretting corrosion of steel [22] and (b) Microscopic surface asperities of two bodies pressure and oscillatory movement form wear debris [23].*

h) Stress-Corrosion cracking

It results from the combined action of a mechanical stress and oxidation reactions [24].

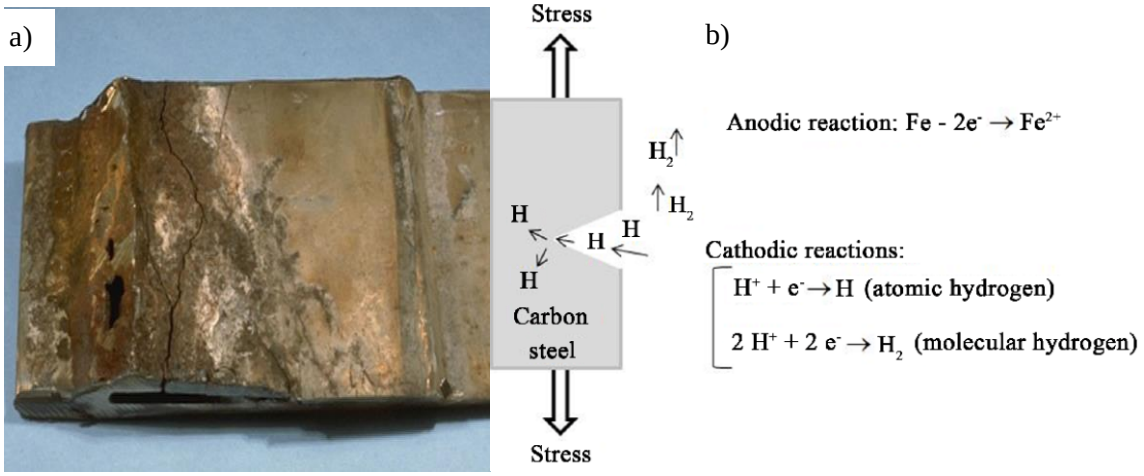

Figure I. 9: *(a) Stress corrosion of a welded alloy steel joint [25] and (b) its mechanism [26].*

i) Corrosion prevention methods

In this section, methods to prevent and minimise corrosion will be presented. It is important to understand the causes of corrosion in order to effectively prevent it. Some common prevention methods include coating the metal surface with protective layers, using cathodic protection, using corrosion inhibitors or controlling the environment in which the metal is exposed. Minimising corrosion can also be achieved through regular maintenance and inspection of the metal surfaces. By implementing these prevention methods, the lifespan of metal structures can be extended and potential safety hazards can be avoided. One of these methods is the corrosion inhibitors, which plays a very important role in lowering the rate of corrosion and extending the lifespan of metal structures and equipment. Therefore, corrosion inhibitors can be defined as: a chemical substance added in low concentration to the metal surfaces that are in corrosive media to reduce the damage that corrosion can do so the material remains good as long as a possible way [27].

Depending on the type of inhibitor and the envirenmont in which it is used, corrosion inhibitors have different mechanisms (figure I.10). Nevertheless, corrosion inhibitors often operate through one or more of the following mechanisms [28]:

Adsorption : The molecular surface charge of the inhibitor is chemically adsorbed (chemisorption) and interacts with the surface charge by forming a protective layer on the metal surface.

Passivation : The reaction and combination between adsorbate and adsorbent (physisorption) lead to the formation of a protective layer.

Form a stable complex : The corrosion inhibitor reacts to the potential corrosive ion present in the electrolyte, and the formation of the product at the electrolyte/metal is complex.

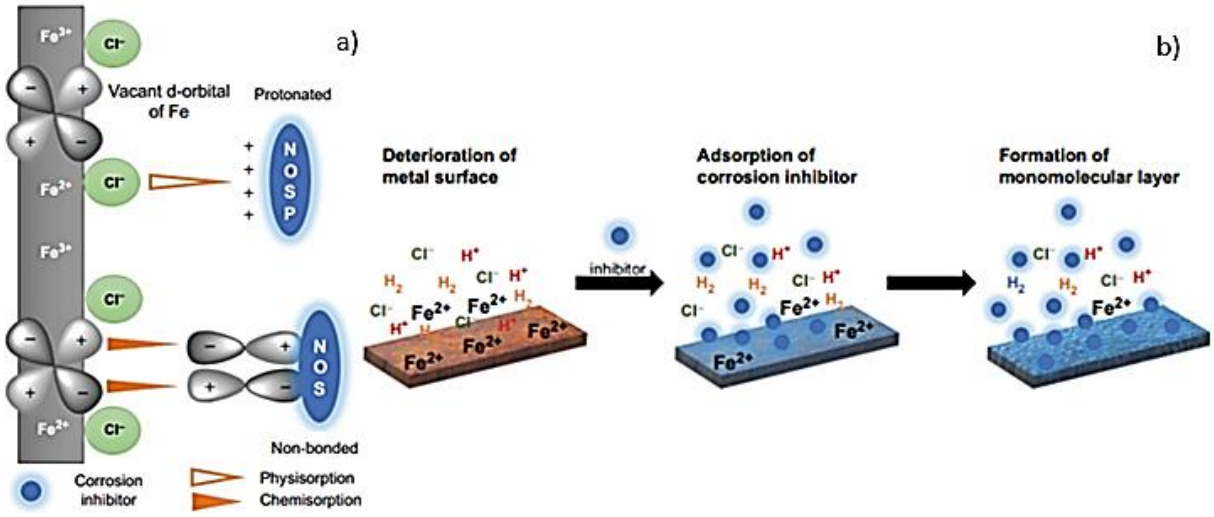

Figure I. 10: *a) Physical and chemical adsorption process, b) Formation of a new protective monolayer on a metal surface [29].*

I.2. Classification of inhibitors

According to different standards and studies corrosion inhibitors are classified into three domains as shown in the figure below [29].

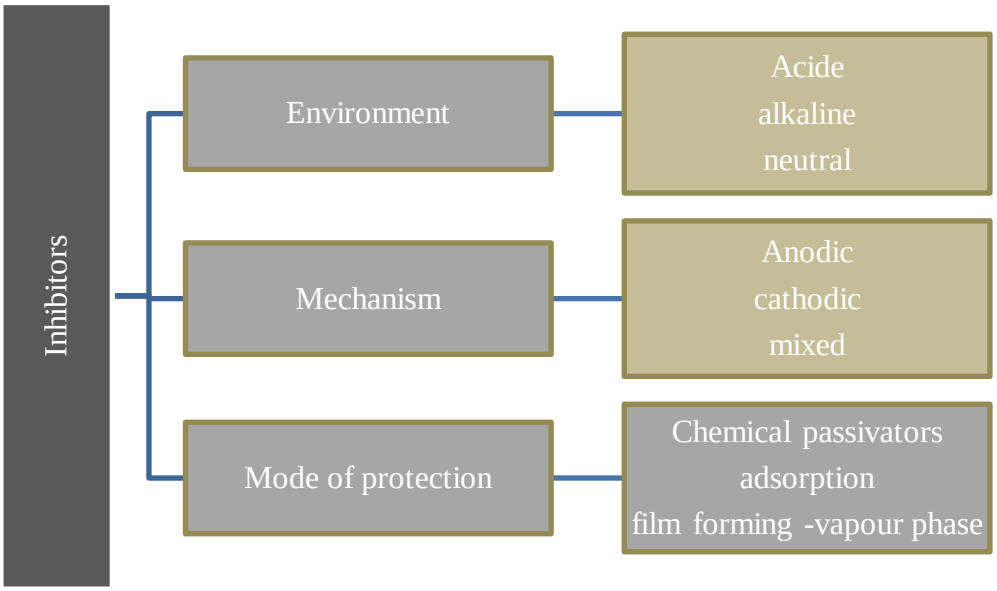

Figure I.11: *Classification of corrosion inhibitors.*

I.2.1. Based on environment

Certain corrosion inhibitors are efficient over a wide pH range, whereas others perform better over a narrower pH range. The specific use and pH of the environment determine which corrosion inhibitor should be used. whether it is organic or inorganic compounds.The formation of a film leads to reducing the attack at a metal such as steel in acid media.

I.2.2. Based on mechanism

These inhibitors can be divided into anodic, cathodic, or mixed-type depending on which electrochemical reactions they are blocking [30] .

I.2.2.1.Anodic inhibitors

Anodic inhibitors increase the potential of the anode by forming a thin protective coating along it, which slows the corrosion reaction [31]. It is worth noting that, Inhibitors of passivation can actually speed up corrosion and induce pitting when concentrations are below necessary limits. Monitoring the inhibitor concentration is crucial due to this [29].

I.2.2.2. Cathodic inhibitors

Essentially, cathodic inhibitors slow down the reduction reaction rate of the electrochemical corrosion cell, which in turn reduces corrosion. As a result, the cathodic sites

are blocked by precipitation. Cathodic inhibitors change the direction of the corrosion potential to anodic. Here, the cations go in the direction of the cathode surfaces, where they are electrochemically or chemically precipitated, blocking those surfaces [29].

I.2.2.3. Mixed inhibitors

As its name implies, it slows both the cathodic and anodic processes involved in corrosion [29].even though they have little influence on the corrosion potential.

I.2.3. Based on mode of protection

I.2.3.1. Chemicals passivators

In order to achieve passivity, chemical passivators have a sufficient equilibrium potential (redox or electrode potential) and a sufficiently low overpotential [29].

I.2.3.2. Adsorption inhibitors

Typically, these are the inhibitors that are used most frequently. As a result, they tend to become adsorbent on the metal surface and cover the entire surface in organic substances [29].

I.2.3.3. Film forming inhibitors

Many compounds referred to as "film forming inhibitors" appear to stop corrosion by generating a blocking or a barrier film of a material different than the actual inhibiting species itself, in contrast to adsorption inhibitors, which form the straightforward adsorbed film of the inhibitory species [32].

I.2.3.4. Vapor phase inhibitors

These are chemicals with a modest but noticeable vapour pressure. The metal, where the inhibitor is adsorbing, is in contact with the vapour at this point. The moisture then causes it to hydrolyze, releasing defence ions with corrosion-inhibiting qualities [29].

I.2.3.5. Volatile inhibitors or vapor phase inhibitors

In a closed environment, volatile corrosion inhibitors (VCIs) transfer to corrosion sites by volatilizing from their sources [29].

I.3. Green corrosion inhibitors

The application of green corrosion inhibitors, which reduce the corrosion rate to the appropriate level with low environmental impact, is one of the key approaches to corrosion control in modern society. From the point of view of environmental compatibility, this area of research is experiencing significant developments. Due to increasing ecological awareness, corrosion inhibitors are now subject to stringent restrictions and regulations enforced by environmental agencies in a number of nations. In recent years, intensive research has been carried out on green corrosion inhibitors made from plants extracts.

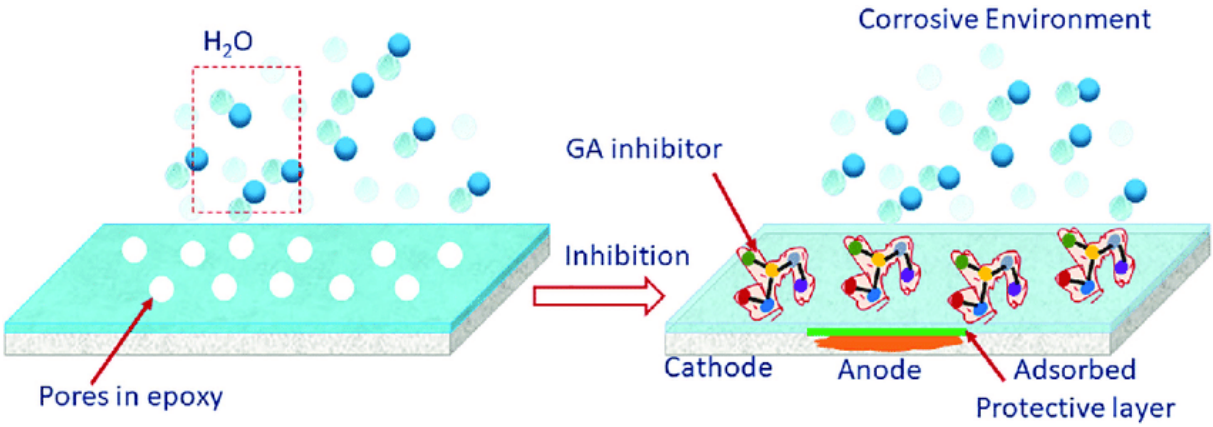

Figure I. 11: *Schematic diagram showing the corrosion inhibition mechanism of GA in the modified.*

Green inhibitors are extensively used to control the corrosion of different types of steels in acidic environments, especially in the oil and gas industry. Based on their chemical nature, green inhibitors can be classified into two groups namely organic and inorganic . Several types of organic green inhibitors include plants (extracts, oil), ionic liquids, amino acids, drugs, and natural polymers.

Literature Review on the plants extracts as green corrosion inhibitors

Due to their low cost, availability, environmental friendliness, and ecological acceptability, green inhibitors have been the focus of recent scientific studies on the protection of metallic materials against corrosion. To protect metal materials from corrosion; a natural extracts have been widely used. The efficiency of these extracts as corrosion inhibitors is commonly evaluated through electrochemical tests. However, the inhibition efficiency of various extract concentrations is a valuable and very important indicator to obtain a clear

outlook of the choice of an extract for a particular purpose. In this study, we focused on the use of green tea extracts (GTE) as corrosion inhibitors.

I.3.1.1. Green tea extracts

According to scientific research published by C. A. Loto in 2011 [33], green tea extract provided effective corrosion inhibition performance at room temperature of the mild steel in 0.2 M and 0.5 M H2SO4 medium. The various percentages of tea extract used produced good results, though the best results were obtained with the 100% extract concentration in the two different sulphuric acid concentrations. It was possible to achieve values of up to 94% inhibitor efficiency at 100% tea extract concentration in 0.5M sulphuric acid and 79% inhibitor efficiency at the same concentration of extract in 0.2 M H2SO4.

GTEs was tested also as a corrosion inhibitor for carbon steel in both HCl and H2SO4 solutions by A.M. Alsabagh et al [34]. It was found that the maximum inhibition efficiency of 81.47% and 71.65% was obtained in 1M HCl and in 0.5M H2SO4, respectevily, at concentration 500 ppm. The corrosion rate was found to decrease with the increases of concentrations while inhibition efficiency increases with increasing concentration of GTEs in both HCl and H2SO4 solutions. On another side, the results presented by SEM analysis confirmed the adsorption of the green tea extract molecules on the carbon steel surface. This suggests that green tea extract could potentially be used as a corrosion inhibitor for carbon steel.

Green tea extract may act as an biodegradable and eco-friendly for inhibiting corrosion of the CS steel in acidic environments. As shown in study by R. Salghi et al. [35], this green tea extract was used as a corrosion inhibitor on the C38 steel (CS) in 1.0 M HCl. The authors obtained that GTE acts essentially as mixed-type inhibitor controlling cathodic and anodic reactions with slight predominant in cathodic branches. Obtained results showed that the inhibition efficiency decreased with a rise in the temperature. Activation energy, entropy and enthalpy of corrosion process were estimated using experimental measurements.

In 2018, A B Hamdan et al. published another study on green inhibitors [36]. They obtained that the efficiency of green (GTE) and black tea extract (BTE) of mild steel in 1M HCl solution increased by increasing these both extracts concentration. In addition, with increasing the bath temperature, the efficiency these plants extracts was decreased. It was reported also that the adsorption behavior of both inhibitors on the mild steel surface obeyed the Langmuir adsorption isotherm and they inhibited the corrosion of mild steel by adsorption mechanism where the adsorption process involved was exothermic, physisorptive and spontaneous. This green extract

performed very well and effective as corrosion inhibitor to slow down the rate of corrosion of mild steel in 1M of HCl solution at which the percentage of inhibitor efficiency is 83.1 and 81.7% for GTE and BTE respectively at 0.25 g/L inhibitor concentration.

On another hand, I. Pradipta et al. were evaluated the aqueous green tea (Camellia sinensis) extract as a corrosion inhibitor on carbon steel in a 3.5 % NaCl corrosive medium [37]. Through linear polarization resistance measurements, the green tea extract exhibited a similar corrosion inhibition efficiency to commercial calcium nitrite corrosion inhibitor at similar concentrations. At equal volumes, the green tea extract exhibited a higher corrosion inhibition efficiency of 75-80%. On the basis of liquid chromatography-mass spectrometry, (-)-epigallocatechin gallate, (-)-epicatechin gallate, and catechin or (-)-epicatechin are supposed to form the mixed-type corrosion inhibiting film.

J-Y. Kim et al.[38] Were studied the inhibitive properties of tea tree extract on mild steel (MS) and 304 stainless steel (STS) immersed in 1 M HCl solution at room temperature. Pitting corrosion and uniform corrosion for STS and for MS at room temperature were retarded, with inhibition efficiencies of 86% and 77%, respectively. The inhibition of pitting and uniform corrosion was confirmed by SEM and LSCM analysis in terms of surface roughness and pitting morphologies. The most effective constituent contributing to the inhibitory performance of tea tree extract was revealed to be α-terpineol, with an inhibition efficiency of 83%. In this study, the anticorrosion mechanism was explained by the formation of organic-Fe complexes on the corroded steel surface via electron donor and acceptor interactions in the presence of an oxygen atom of the hydroxyl group or ether of organic inhibitors.

I.3.1.2. Carrot extracts

Carrot extract is another plant extract that prevents corrosion; it was developed by a number of researchers, including:

R. Ihamdane et al. [39] were studied the effect of the essential oil (EO) of the aerial part of Daucus carota L as an inhibitor for mild steel in 1 M HCl. the experimental results show that the EO act as an effective inhibitor for mild steel in acidic solution, and their effectiveness increases with their concentration. On the other hand, the polarization plots indicate that the studied EO inhibits the evolution of the cathodic and anodic reaction. In the presence of inhibitor, the charge transfer resistance (Rct) increases and double-layer capacitance (Cdl) decreases. Moreover, the studied EO inhibits the corrosion process by adsorbing on the mild steel surface, and their adsorption mode followed Langmuir adsorption isotherm.

In a study by M.T. Saeed et al.[40], the effect of the carrot (Daucus carota L.) peels (CP) extract on the corrosion of mild steel in 1M HCl solution was investigated. The increase in temperature has a great influence on the corrosion rate; it accelerates the corrosion process significantly. It is important to consider the temperature factor when designing materials and structures to ensure their longevity and safety. At studied temperatures, the increase in the concentration of CP extract was reduced the substantial reduction in CR. However, the increase in the CR at each CP extract along with the increase in the temperature tallied to the increase in kinetic activities at the electrolyte and metal interface. Results show that with the increase of 0.5 g/l CP extract, about 3 times lower CR of mild steel at studied temperatures than in pure 1M HCl solution affirm its robust inhibitive efficiency. On the other hand, the restricted dissolution of mild steel is confirmed by a large change in anodic Tafel slope and a gradual decline in CR with increasing CP extract concentration. The authors were also found that the chemisorption, a layer of inhibitor material, is responsible for high IE and the Freundlich Isotherm is best fitted, with correlation coefficients reaching unity.

Another study on the influence of Daucus carota aerial part extract (DCA) on the corrosion inhibition of mild steel in 1N hydrochloric acid solution was carried out by V. Kavitha et al.[41]. They are achieved that the maximum inhibition efficiency of 95.72% is obtained at 2% of DCA extract at 5h of immersion at 30°C. DCA adsorbed on the mild steel surface follows Temkin adsorption isotherms. This suggests that the adsorption of DCA on mild steel surface is a physical process and the adsorption energy decreases with increasing surface coverage. The inhibition efficiency increases with increase in concentration of the inhibitor and time of immersion. On the other side, theoretical analysis with quantum chemical method results revealed that β-carotene possess corrosion inhibition property on surface of mild steel by adsorption process. Weight loss measurements and phytochemical screening showed that DCA acts as mixed type inhibitor and adsorb on the metal surface to protect against corrosion.

References

[1] V. S. Sastri, ' *Green corrosion inhibitors: theory and practice*'. John Wiley & Sons, 2012.
[2] 'A corroded hinge'. Accessed: Apr. 16, 2023.
[3] 'factors.htm'. Accessed: Apr. 26, 2023. [Online]. Available: https://corrosion-doctors.org/Corrosion-Factors-Cells/factors.htm
[4] P. Guraieb and Q. Wang, 'Corrosion and scale at high pressure high temperature', *Trends Oil Gas Corros. Res. Technol.*, pp. 431–451, 2017.
[5] M. Kutz, '*Handbook of environmental degradation of materials*'. William Andrew, 2018.
[6] C. Verma, '*Handbook of science and engineering of green corrosion inhibitors*': *modern theory, fundamentals and practical applications*. Amsterdam, Netherlands: Elsevier, 2022.
[7] L. E. Umoru, A. A. Afonja, and B. Ademodi, 'Corrosion Study of AISI 304, AISI 321fp, vol. 07, no. 04, pp. 291–299, 2008.
[8] M. Tavakkolizadeh and H. Saadatmanesh, 'Galvanic corrosion of carbon and steel in aggressive environments', *J. Compos. Constr.*, vol. 5, no. 3, pp. 200–210, 2001.
[9] 'File:Stainless-steel-mild-steel_cropped.jpg'. Accessed: Apr. 17, 2023. [Online]. Available:https://commons.wikimedia.org/wiki/File:Stainless-steel-mild-steel_cropped.jpg
[10] N. Corlett, L. E. Eiselstein, and N. Budiansky, 'Crevice Corrosion', in *Shreir's Corrosion*, Elsevier, pp. 753–771, 2010.
[11] 'caverneuse_2_zoom.jpg'. Accessed: Apr. 18, 2023. [Online]. Available: https://www.cdcorrosion.com/mode_corrosion/corrosion_image/caverneuse_2_zoom.jpg
[12] 'caverneuse_1_zoom.jpg'. Accessed: Apr. 26, 2023. [Online]. Available: https://www.cdcorrosion.com/mode_corrosion/corrosion_image/caverneuse_1_zoom.jpg
[13] T. Dawson, V. Johnson, P. Miller, M. Morabito, and G. W. Swain, 'EN380 Naval Material Science and Engineering Course Notes'2022.
[14] 'what-is-pitting-corrosion'. Accessed: Apr. 26, 2023. [Online]. Available: https://www.ddcoatings.co.uk/2276/what-is-pitting-corrosion
[15] 'pitting-corrosion'. Accessed: Apr. 19, 2023. [Online]. Available: https://www.merusonline.com/pitting-corrosion/
[16] Z. Ahmad, 'Types of corrosion', in *Principles of Corrosion Engineering and Corrosion Control*, Elsevier, pp. 120–270, 2006.
[17] E. L. Colvin, 'Aluminum Alloys: Corrosion', in *Encyclopedia of Materials: Science and Technology*, Elsevier, pp. 107–110, 2001.
[18] M. Sedlak Mosesson, 'Modelling of intergranular stress corrosion cracking mechanism: Du som saknar dator/datorvana kan kontakta alfred@ kth. se för information', 2020.
[19] 'erosion-corrosion-mechanism-factors-prevention'. Accessed: My 08, 2023. [Online]. Available: https://melezy.com/erosion-corrosion-mechanism-factors-prevention/
[20] M. Güner and M. M. Özbayer, 'wear and its effects in centrifugal pumps', *Üzüncü Il Üniversitesi Tarım Bilim. Derg.*, vol. 29, no. 3, pp. 569–582, 2019.
[21] T. S. N. Sankara Narayanan, 'Nanocoatings to improve the tribocorrosion performance of materials', in *Corrosion Protection and Control Using Nanomaterials*, Elsevier, pp. 167–212? 2012.
[22] 'frottement_zoom.jpg'. Accessed: Apr. 26, 2023. [Online]. Available: https://www.cdcorrosion.com/mode_corrosion/corrosion_image/frottement_zoom.jpg
[23] '1367-an-overview-of-fretting-wear'. Accessed: Apr. 26, 2023. [Online]. Available: https://www.powertransmission.com/articles/1367-an-overview-of-fretting-wear
[24] T. Shoji, Z. Lu, and Q. Peng, 'Factors affecting stress corrosion cracking (SCC) and fundamental mechanistic understanding of stainless steels', in *Stress corrosion cracking*, Elsevier, pp. 245–272, 2011.

[25] 'SCC2_zoom.jpg'. Accessed: Apr. 26, 2023. [Online]. Available: https://www.cdcorrosion.com/mode_corrosion/corrosion_image/SCC2_zoom.jpg
[26] F. B. Mainier, P. C. F. Almeida, B. Nani, L. H. Fernandes, and M. F. Reis, 'Corrosion caused by sulfur dioxide in reinforced concrete', *Open J. Civ. Eng.*, vol. 5, no. 04, p. 379, 2015.
[27] A. Miralrio and A. Espinoza Vázquez, 'Plant extracts as green corrosion inhibitors for different metal surfaces and corrosive media: a review', *Processes*, vol. 8, no. 8, p. 942, 2020.
[28] I. W. Ma, S. Ammar, S. S. Kumar, K. Ramesh, and S. Ramesh, 'A concise review on corrosion inhibitors: types, mechanisms and electrochemical evaluation studies', *J. Coat. Technol. Res.*, pp. 1–28, 2022.
[29] G. Palanisamy, 'Corrosion inhibitors', *Corros. Inhib.*, pp. 1–24, 2019.
[30] L. K. M. O. Goni and M. A. J. Mazumder, 'Green Corrosion Inhibitors', in *Corrosion Inhibitors*, A. Singh, Ed., IntechOpen, 2019.
[31] A. Al-Mayout, A. Al-Suhybani, and A. Al-Ameery, 'Corrosion inhibition of 304SS in sulfuric acid solutions by 2-methyl benzoazole derivatives', *Desalination*, vol. 116, no. 1, pp. 25–33, 1998.
[32] M. Abdallah and B. Jahdaly, 'Gentamicin, kanamycin and amikacin drugs as non-toxic inhibitors for corrosion of aluminum in 1.0 M hydrochloric acid', *Int J Electrochem Sci*, vol. 10, pp. 9808–9823, 2015.
[33] C. A. Loto, 'Inhibition effect of Tea (Camellia Sinensis) extract on the corrosion of mild steel in dilute sulphuric acid', 2011.
[34] A. M. Alsabagh, M. A. Migahed, M. Abdelraouf, and E. A. Khamis, 'Utilization of Green Tea as Environmentally Friendly Corrosion Inhibitor for Carbon Steel in acidic media', *Int J Electrochem Sci*, vol. 10, 2015.
[35] Laboratory of Applied Chemistry and Environment, ENSA, University Ibn Zohr, PO Box 1136.Agadir, Morocco and R. Salghi, 'Inhibition of C-steel Corrosion by Green Tea Extract in Hydrochloric Solution', *Int. J. Electrochem. Sci.*, pp. 3283–3295, Apr. 2017.
[36] L. E. Yahaya, S. O. A. Royeun, S. O. Ogunwolu, C. O. Jayeola, and R. O. Igbinadolor, 'Green and Black Tea (Camellia sinensis) Extracts as Corrosion Inhibitor for Mild Steel in Acid Medium', *Env. Sci*, 2017.
[37] I. Pradipta, D. Kong, and J. B. L. Tan, 'Natural organic antioxidants from green tea form a protective layer to inhibit corrosion of steel reinforcing bars embedded in mortar', *Constr. Build. Mater.*, vol. 221, pp. 351–362, Oct. 2019.
[38] J.-Y. Kim, I. Shin, and J.-W. Byeon, 'Corrosion Inhibition of Mild Steel and 304 Stainless Steel in 1 M Hydrochloric Acid Solution by Tea Tree Extract and Its Main Constituents', *Materials*, vol. 14, no. 17, p. 5016, Sep. 2021.
[39] R. Ihamdane *et al.*, 'The Inhibition Effect of Aerial Part of Daucus carota L Essential Oil on the Corrosion Performance of Mild Steel in HCl Medium', 2021.
[40] M. T. Saeed, M. Saleem, A. H. Niyazi, F. A. Al-Shamrani, N. A. Jazzar, and M. Ali, 'Carrot (Daucus carota L.) peels extract as an herbal corrosion inhibitor for mild steel in 1M HCl solution', *Mod. Appl. Sci.*, vol. 14, no. 2, pp. 97–112, 2020.
[41] V. Kavitha and D. N. Gunavathy, 'Evaluation of Daucus Carota aerial extract as corrosion inhibitor of mild steel in hydrochloric acid medium', *Int. J. Res. Advent Technol.*, vol. 2, no. 7, pp. 146–154, 2014.

Chapter 2

Computational methods in quantum chemistry

II.1. Introduction

In this chapter, we provide a concise overview of several quantum mechanical methods, as well as their associated theorems, along with the hybrid functional B3lyp.and the most important quantum reactivity descriptors which play a pivotal role in understanding chemical reactivity at the quantum level.

II.2. Shrodinger equation

The Schrödinger equation was formulated in 1926 by the Austrian physicist Erwin Schrödinger[1].It describes how a physical system's quantum state changes over time. Also known as a state vector or wave function. The Schrödinger equation and its variants are often used in the study of partial differential equations in pure mathematics. Used in geometry, spectral, integral systems…[2].And in various branches of physics, chemistry, and engineering where quantum effects are significant.

For a general quantum system:

$$i\hbar \frac{\partial}{\partial t}\Psi = \hat{H}\,\Psi \qquad \textit{Eq. II. 1}$$

Where

- Ψ is the wave function
- $i\hbar\frac{\partial}{\partial t}$ is the energy operator
- i is the imaginary unit and ħ is the plank constant.
- $\hat{H}$ is the Hamiltonian operator.

In the context where the molecular Hamiltonian is denoted as "Ĥ", the total energy operator captures the essence of the system under study. From this operator, the total energy (E) and the wave function (ψ) can be derived, encompassing all the pertinent information regarding the system. The total Hamiltonian Ĥ, formulated in atomic units, incorporates the following components:

$$\hat{H} = \widehat{T_n} + \widehat{T_e} + \widehat{V_{ee}} + \widehat{V_{nn}} + \hat{V}_{ne} \qquad \textit{Eq. II. 2}$$

where $\mathbf{T}_e$ and $\mathbf{T}_n$ are respectively kinetic energy operators of N electrons and n nuclei $\mathbf{V}_{ee}$ and $\mathbf{V}_{nn}$ are respectively inter-electronic and internuclear electrostatic repulsion energy operators and is not the electrostatic attraction energy operator nuclei-electrons.

$$\widehat{T_e} = \sum_{i=1}^{N}(-\frac{1}{2}\nabla_{ri}^2) \qquad \textit{Eq. II. 3}$$

$$\widehat{T_n} = \sum_{\alpha=1}^{N}(-\frac{1}{2}\nabla_{r\alpha}^2) \qquad \textit{Eq. II. 4}$$

$$\widehat{V_{ee}} = \sum_{i=1}^{N-1}\sum_{j>i}^{N}\frac{1}{r_{ij}} \qquad \textit{Eq. II. 5}$$

$$\widehat{V_{ne}} = -\sum_{\alpha=1}^{n}\sum_{i=i}^{N}\frac{Z_\alpha}{r_{i\alpha}} \qquad \textit{Eq. II. 6}$$

The variables Zα and Zβ represent the respective atomic numbers associated with the α and β nuclei, while rαβ denotes the internuclear distance. In the realm of quantum chemistry, the processing of all molecular interactions is a complex task, as the Schrödinger equation cannot be directly solved with high accuracy. This is primarily due to the fact that the potential experienced by each electron or nucleus is influenced by the collective motion of all the electrons and nuclei within the system. Consequently, the utilization of approximations becomes indispensable. Two key approximations have been developed to address this challenge, enabling the simplification of this intricate problem.The two fundamental approximations, namely the Born-Oppenheimer approximation[3], and the orbital approximation [4], play a seminal role in the inception of electronic structure calculations. These approximations, which have their origins in quantum chemistry, have paved the way for the initial computations pertaining to the electronic structure of molecules.

II.2.1 Born-Oppenheimer's hypothesis

Due to the significant disparity in mass between nuclei and electrons, it is widely recognized that the motion of nuclei is considerably slower compared to that of electrons. As a consequence, it becomes feasible to separate or decouple the motion of electrons from that of the positively charged nuclei. In the study of molecular electron dynamics, the nuclei are treated as nearly stationary entities, while the focus lies on investigating the movement of electrons within the molecule. The molecular wave function can therefore be written as follows:

$$\Psi_{mol} = \Psi_{ele}.\Psi_{nucl} \qquad \textit{Eq. II. 7}$$

In this context, the electronic Hamiltonian is expressed by the following equation:

$$\widehat{H}_{ele} = \sum_{i=1}^{N}(-\frac{1}{2}\nabla_{ri}^{2}) - \sum_{\alpha=1}^{n}\sum_{i=i}^{N}\frac{Z_\alpha}{r_{i\alpha}} + \sum_{i=1}^{N-1}\sum_{j>i}^{N}\frac{1}{r_{ij}} \qquad \textit{Eq. II. 8}$$

It is then possible to write the Schrödinger equation for the electron as:

$$\widehat{H}.\Psi_{ele} = E_{ele}.\widehat{\Psi}_{ele} \qquad \textit{Eq. II. 9}$$

II.2.2. orbital approximation

However, solving the Schrödinger equation becomes challenging due to the intricate interactions among electrons. The orbital approximation has been instrumental in simplifying this task by considering the wave function of the electronic system, denoted as Ele, as the product of single-particle wave functions Φ:

$$\Psi_{ele}(r_1\, r_2 \dots\dots\dots\dots r_N) = \Phi_1(r_1)\Phi_2(r_2)\dots\dots\Phi_N(r_N) \qquad \textit{Eq. II. 10}$$

However, it is important to note that this wave function does not adhere to the Pauli exclusion principle[5]. The Pauli exclusion principle dictates that the wave function describing a multi-electronic system must exhibit a change in spin upon swapping the coordinates of any two electrons. In the orbital approximation, the wave function that satisfies this principle adopts the structure of a Slater determinant[6]. The latter respects Pauli's principle in its generalized form which specifies that identical fermions must not have the same quantum number. The new function wave is written as follows:

$$\Psi = \frac{1}{\sqrt{n!}}\begin{bmatrix} \emptyset_1(\chi_1) & \cdots & \emptyset_n(\chi_1) \\ \vdots & \ddots & \vdots \\ \emptyset_1(\chi_n) & \cdots & \emptyset_n(\chi_n) \end{bmatrix} \qquad \textit{Eq. II. 11}$$

Where N is the number of electrons and $\frac{1}{\sqrt{n!}}$ Is the normalization factor.

Several quantum methods are used to solve the Schrödinger equation, like HF (Hartree-Fock)[5,7], or density functional theory (DFT), this latter which uses electronic density as the only variable (in addition to the spin) and takes into account electronic

correlation, remains the best alternative as it is less costly in time of calculation and gives satisfactory results (correct reproduction of the physicochemical properties of molecular systems, with in particular a good agreement between DFT geometries and X structures).

II.3. Density functional theory

In the field of quantum mechanics, Density Functional Theory (DFT) has been immensely successful in describing ground-state quantum properties of the matter (from atoms to extended solids). Its success in computational chemistry is due to the fact that the energy of any N-electron system can be expressed as a functional of the ground-state electronic density ρ- from which any other ground-state property can be derived and that-ρ is uniquely determined by a given external potential[8].

II.3.1. Principle of the DFT method

It consists of replacing the resolution of the multi-body problem with that of the single-body problem in an effective field taking into account all interactions. Its aim is to find a functional way to connect density with energy. The postulate asserts that the energy of a system composed of multiple electrons can be succinctly expressed by means of the electronic density which allows the latter to be used instead of the wave function in order to calculate energy. The wave function of a N electron system depends on 3N space coordinates (x, y, z) and N spin coordinates on the other hand, the electronic density depends only on the three space coordinates and the electron's spin coordinate. The primary goal of the Density Functional Theory (DFT) method is to establish the functional expressions $T_e[\rho]$, $V_{ee}[\rho]$, and $V_{ne}[\rho]$ based on the electronic density ρ(r)[9,10]. Consequently, the functional representing the total energy is formulated in the ensuing manner.

$$E[\rho] = \hat{T}_e[\rho] + \hat{V}_{ee}[\rho] + \hat{V}_{ne}[\rho] \qquad \textit{Eq. II. 127}$$

The formalism of the Density Functional Theory (DFT) method is grounded upon the fundamental theorems proposed by Hohenberg and Kohn [11].

II.3.1.1. Hohenberg-Kohn theorems

The many-electron wave-function is a function of 3N variables and is too complicated

to deal with. Hohenberg and Kohn[12], proved two theorems that enable the electron density to be used instead. This is a far simpler quantity to deal with as it only depends on 3 variables, the spatial coordinates:

Theorem 1

The external potential Vext(r) is, to within a constant, a unique functional of the electronic density ρ(r). Since in turn Vext(r) fixes $\hat{H}$, it is seen that the full many-particle ground state is a unique functional of ρ(r).

So the Hamiltonian and hence all the properties of a system are determined uniquely by the system's electron density. This suggests that recasting the Hamiltonian in terms of ρ(r) would be a good idea[13].

Theorem 2

For a trial ρ(r) that satisfies the boundary conditions $\tilde{n}(r) \geq 0$ and $\int \tilde{n}(r)d^3 r = N$ and is associated with a $\tilde{V}$ ext, the energy it gives is an upper bound to the true energy E0.

This theorem states that the energy of the system is variational with respect to the density, $E[n^0(r)] \leq E[\tilde{n}(r)]$. That is, the lowest energy is for the ground state density and any other density results in a higher energy[13].

II.3.1.2. Kohn-Sham Approach:

Similar to the Hartree-Fock method, the Kohn-Sham approach, guided by the Hohenberg and Kohn theorem, revolves around the resolution of monoelectronic problems to address the behavior of electrons within a non-homogeneous system. In this theory, an artificial system comprising 18 independent electrons is employed, subject to an average effective field. The potential Veff is precisely tailored to ensure that the electronic density of this fictitious system perfectly matches that of the actual system. The solution of the Schrödinger equation within this framework is pursued accordingly, The methodology entails the utilization of orthonormal monoelectronic spatial functions, denoted as Kohn-Sham orbitals, to solve the problem. The electronic density of the artificial system is subsequently constructed by aggregating the probabilities associated with each monoelectronic component. This approach facilitates the preliminary assessment of the electronic kinetic energy. The disparity from the actual electronic kinetic energy is attributed to the term that remains unknown, namely the exchange and

correlation energy Exc[ρ(r)]. This term is incorporated within the expression of the universal functional in accordance with the Hohenberg and Kohn formulation.

$$V_{eff}[\rho(r)] = V_{ext}(r) + V_{xc}[\rho(r)] + \int \frac{\rho(r')}{|r-r'|} dr' \qquad \textit{Eq. II. 83}$$

Vxc[ρ(r)] is the exchange-correlation potential, functional derivative of Exc[ρ(r)] in relation to the density ρ(r) and the conventional electron-electron potential ($\int \frac{\rho(\acute{r})}{r-\acute{r}} d\acute{r}$) [14].

This process incorporates the diminishing electronic density across space, prompted by the existence of an electron at a specific location. By doing so, it enables the precise inclusion of exchange-correlation effects in the overall energy calculation. This effective potential is employed in the Schrödinger's equations for the mono-electronic system, the resolution of which yields the mono-electronic wave functions. These wave functions, upon summation of their squares, provide access to the density.

$$\rho(r) = 2\sum_{i=1}^{n_e/2} \left|\emptyset_{i/2}\right|^2 \qquad \textit{Eq. II. 94}$$

II.3.2. Main functions used in DFT

The success of Density Functional Theory (DFT) can be attributed to several approximations, all of which revolve around the exchange-correlation functional. These approximations are typically denoted, in practice, by a combination of letters representing the initials of the authors. The first part of the abbreviation pertains to the calculation method for the exchange term, while the second part corresponds to the correlation term.

II.3.2.1. Approximation of the local density

The primary challenge in the development of the Kohn-Sham formalism resides in constructing exchange-correlation functions. The foundation of all contemporary exchange-correlation functions lies in the local approximation of density known as Local Density Approximation (LDA). LDA involves regarding the density function at a given point as locally defined and constant. It is mathematically defined as follows:

$$E_{xc}^{LDA}[\rho(r)] = \int \rho(r)\, \varepsilon_{xc}\big(\rho(r)\big) dr \qquad \textit{Eq. II. 105}$$

The Local Density Approximation (LDA) stems from the concept of a uniform electron gas, where the term εxc(ρ(r)) denotes the exchange energy that arises from the correlation of

particles within the uniform gas of density ρ(r). This exchange energy can be regarded as the combined effect of an exchange contribution and a correlation contribution:

$$\varepsilon_{xc}\big(\rho(r)\big) + \varepsilon_x\big(\rho(r)\big) + \varepsilon_c(\rho(r)) \qquad \textit{Eq. II. 116}$$

The exchange term εx(ρ(r)) proposed by Dirac[15,16], is known exactly:

$$\varepsilon_x\big(\rho(r)\big) = -\frac{3}{4}\left(\frac{3\rho(r)}{\pi}\right)^{1/3} \qquad \textit{Eq. II. 127}$$

For the correlation energy εc(ρ(r)), no exact analytical form is known. Several configurations have been proposed, the most elaborate are those of Perdew and Zinger[17], and Perdew and Wang[18],but the most used functional approach is the one proposed by Vosko and collaborators[19]. It is based on an interpolation of the results of very precise quantum MonteCarlo calculations on a uniform electron gas made by Ceperley and Alder[20].

This approximation has been extended to spin-free systems. It is known as LSDA (Local Spin Density Approximation). The functional exchange-correlation, in this case, separates the densities of spin α and β. It is written in the form:

$$E_{xc}^{LSD}\big[\rho_\alpha(r), \rho_\beta(r)\big] = \int \rho(r)\, \varepsilon_{xc}(\rho_\alpha(r)\rho_\beta(r))dr \qquad \textit{Eq. II. 138}$$

In practice, this approximation tends to overestimate bond energies, leading to shorter bond lengths. Nevertheless, it remains effective and yields favorable properties for atoms and molecules.

II.3.2.2. Generalized gradient approximation:

To enhance the precision of DFT calculations and address the limitations of the LDA and LSDA methods, it becomes imperative to develop more refined approximations for the exchange-correlation function. Generalized Gradient Approximation (GGA)[21], takes into account the inhomogeneity of the electron density inconsidering exchange-correlation functions depending not only on the density at each point, but also on its gradient. The Exc energy takes a general form similar to that of the LDA:

$$E_{xc}^{GGA} = \int \varepsilon_{xc}^{GGA}\,(\rho(r)\nabla\rho(r))dr \qquad \textit{Eq. II. 19}$$

In practical terms, functionals of this nature treat the exchange and correlation components separately. These functionals, known as non-local NLD (Non-Local Density) functionals, serve as corrective terms to local functionals. By doing so, they effectively rectify the Exc (Exchange-Correlation) energy.

Among the best known and most used are the exchange functionals of Becke (B88) [20], and Perdew and Wang (PW91) [22]; and for the correlation the functionals of Perdew (P86) [23],and that of Lee, Yang and Parr (LYP) [24]. All these functionals allow an improvement at the level of bond energies and geometries of the systems studied with respect to the LDA.

II.3.2.3 Hybrid functional(B3lYP)

Hartree-Fock exchange expressions and DFT exchange-correlation functionals. However, currently one of the most advanced commonly used work-horse functionals, is the B3LYP functional especially for organique molecules [21,[25].

which mix of DFT and HF, and regroup the exchange and correlation parts of the both methods, the aim of functionals for instance the B3LYP is to eliminate some of DFT's most significant problems, such as the self-interaction error[26,27].

$$E_{XC}^{B3LYP} = E_X^{LDA} + a_0(E_X^{HF} - E_X^{LDA}) + a_X(E_X^{GGA} - E_X^{LDA}) + E_C^{LDA} + a_C(E_C^{GGA} - E_C^{LDA}) \quad \text{Eq. II. 140}$$

Where E_X^{GGA} and $E_C^{GGA}$are the generalized gradient approximation exchange and correlation functionals,E_C^{LDA} is the local density approximation to the correlation functionaL,a_0 is set to 0.20,α_x is set to 0.72 a_c is set to 0.81.

II.4. Global reactivity descriptors

Theoretical chemists use reactivity descriptors to describe the behavior of chemical substances during chemical reactions. These descriptors are generally considered to be based on information about the electronic structure and chemical properties of molecules, and can provide valuable information regarding the likely outcome of different chemical reactions.

II.4.1. Ionization potential (I)and The electronic affinity (A).

Ionization potential which is the amount of energy needed to remove an electron from a molecule. High ionization energy indicates high stability and chemical inertness and small ionization energy indicates high reactivity of the atoms and molecules. The electronic affinity wich is defined as the energy released when an electron is added to a neutral molecule. A molecule with high (A) values tend to take electrons easily[28].

(I) and (A) values can be correlated with the Frontier orbitals by the relation:

$I = -E_{HOMO}$ and $A = -E_{LUMO}$

II.4.2. Electro-philicity (ω)

Electro-philicity (ω) gives an idea of the stabilization energy when the system gets saturated by electrons, which come from the external environment. These reactivity information shows if a molecule is capable of donating charge. A good, more reactive, nucleophile is characterized by a lower value of (ω), while higher values indicate the presence of a good electrophile[29].

$$\omega = \frac{\mu^2}{2\eta} \qquad \textit{Eq. II. 151}$$

II.4.3. Chemical potential (μ)

Chemical potential (μ) measures the escaping tendency of an electron and it can be associated with the molecular electronegativity[30].

$$\mu = -\chi = \frac{1}{2}(E_{LUMO} + E_{HOMO}) \qquad \textit{Eq. II. 162}$$

II.4.4. Electro-negativity (χ)

Electro-negativity (χ) representing the ability of molecules to attract electrons [28].

$$\chi = -\frac{1}{2}(E_{LUMO} + E_{HOMO}) \qquad \textit{Eq. II. 173}$$

II.2.5. Hardness (η) and softness (S)

Useful parameters for understanding the behavior of chemical systems. A hard molecule has a large energy gap and a soft molecule has a small energy gap[31].

$$\eta = \frac{1}{2}(E_{LUMO} - E_{HOMO}) \qquad \textit{Eq. II. 184}$$

$$s = \frac{1}{2\eta} \qquad \textit{Eq. II. 195}$$

II.5. Computational and Visualization softwares:

II.5.1. Hyperchem

Hyperchem is a commercial molecular modeling program for Windows that is easily accessible to beginning students. It includes molecular mechanics using several force fields, together with semi-empirical and ab initio quantum mechanical calculations. Molecules may be presented as stick, ball and stick, space-filling, or dotted surface models. Molecular orbitals may be displayed as two-dimensional contour maps or as three-dimensional isodensity surfaces. UV and IR spectra are presented as spectral displays and individual vibrational modes are animated. Hyperchem reads PDB (ENT) files as well as its own HIN format files. One of the strengths of Hyperchem is that it can be driven with internal scripts as well as DDE/OLE interaction with other Windows programs. A freely-distributed web browser plug-in supports manipulable 3-D views of molecules generated by Hyperchem[32].

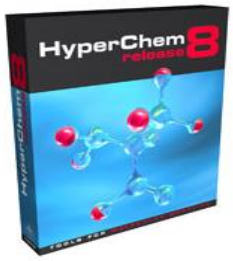

II.5.2. Gaussian

Gaussian is the "industry standard" for ab initio molecular computation of energies, molecular structures, and vibrational frequencies -- along with numerous molecular properties that are derived from these three basic computation types -- for systems in the gas phase and in solution. Additional basis sets and computation types are constantly being added[33].

II.5.3. Gaussian view

a full-featured graphical user interface for Gaussian 98 (Unix or Windows). With the molecule building facility one can quickly and efficiently construct molecular systems. Gaussian calculations can be initiated and monitored from the GaussView and when a calculation has completed, you can use GaussView to examine a variety of results graphically via its advanced visualization facilities[34].

References

[1] T. Britannica, 'Editors of encyclopaedia', *Argon Encycl. Br.*, 2020.
[2] A. Iqbal, 'some aspects on the schrödinger equation', 2012.
[3] H. Djouama, 'Aspects structuraux et électroniques de complexes organométalliques alcynyles luminescents', 2018.
[4] M. Bouzgou, 'Effet du substituant chlorure sur l'extraction liquide-liquide des métaux de transitions par la N-(2-hydroxybenzylidène) aniline', 2019.
[5] D. R. Hartree, 'The wave mechanics of an atom with a non-Coulomb central field. Part I. Theory and methods', presented at the Mathematical Proceedings of the Cambridge Philosophical Society, Cambridge university press, pp. 89–110, 1928.
[6] J. C. Slater, 'The theory of complex spectra', *Phys. Rev.*, vol. 34, no. 10, p. 1293, 1929.
[7] P. Lykos and G. Pratt, 'Discussion on the Hartree-Fock approximation', *Rev. Mod. Phys.*, vol. 35, no. 3, p. 496, 1963.
[8] D. Presti, 'Quantum computational methodologies for the study of molecular crystals', 2015.
[9] L. H. Thomas, 'The calculation of atomic fields', presented at the Mathematical proceedings of the Cambridge philosophical society, Cambridge University Press, pp. 542–548, 1927.
[10] P. A. Dirac, 'Note on exchange phenomena in the Thomas atom', presented at the Mathematical proceedings of the Cambridge philosophical society, Cambridge University Press, pp. 376–385, 1930.
[11] P. Hohenberg and W. Kohn, 'Density functional theory (DFT)', *Phys Rev*, vol. 136, no. 1964, p. B864, 1964.
[12] P. Hohenberg, W. Kohn, and L. Sham, 'The beginnings and some thoughts on the future', in *Advances in Quantum Chemistry*, Elsevier, pp. 7–26, 1990.
[13] A. M. P. Sena, 'Density functional theory studies of surface interactions and electron transfer in porphyrins and other molecules', 2010.
[14] J. Harris and R. Jones, 'The surface energy of a bounded electron gas', *J. Phys. F Met. Phys.*, vol. 4, no. 8, p. 1170, 1974.
[15] J. C. Slater, 'A simplification of the Hartree-Fock method', *Phys. Rev.*, vol. 81, no. 3, p. 385, 1951.
[16] J. P. Perdew and A. Zunger, 'Self-interaction correction to density-functional approximations for many-electron systems', *Phys. Rev. B*, vol. 23, no. 10, pp. 5048–5079, May 1981.
[17] J. P. Perdew and Y. Wang, 'Accurate and simple analytic representation of the electron-gas correlation energy', *Phys. Rev. B*, vol. 45, no. 23, p. 13244, 1992.
[18] S. H. Vosko, L. Wilk, and M. Nusair, 'Accurate spin-dependent electron liquid correlation energies for local spin density calculations: a critical analysis', *Can. J. Phys.*, vol. 58, no. 8, pp. 1200–1211, 1980.
[19] D. M. Ceperley and B. J. Alder, 'Ground State of the Electron Gas by a Stochastic Method', *Phys. Rev. Lett.*, vol. 45, no. 7, pp. 566–569, Aug. 1980.
[20] J. P. Perdew, K. Burke, and Y. Wang, 'Erratum: Generalized gradient approximation for the exchange-correlation hole of a many-electron system, *Phys. Rev. B*, vol. 57, no. 23, p. 14999, 1998.
[21] A. D. Becke, 'Density-functional thermochemistry. I. The effect of the exchange-only gradient correction', *J. Chem. Phys.*, vol. 96, no. 3, pp. 2155–2160, 1992.

[22] A. D. Becke, 'Density-functional exchange-energy approximation with correct asymptotic behavior', *Phys. Rev. A*, vol. 38, no. 6, p. 3098, 1988.
[23] I. Makkonen, M. Hakala, and M. Puska, 'Calculation of valence electron momentum densities using the projector augmented-wave method', *J. Phys. Chem. Solids*, vol. 66, no. 6, pp. 1128–1135, 2005.
[24] J. P. Perdew, 'Density-functional approximation for the correlation energy of the inhomogeneous electron gas', *Phys. Rev. B*, vol. 33, no. 12, p. 8822, 1986.
[25] A. D. Beeke, 'Density-functional thermochemistry. The role of exact exchange', *J Chem Phys*, vol. 98, no. 7, pp. 5648–6, 1993.
[26] A. Sebetci, 'New minima for the Pt8 cluster', *Comput. Mater. Sci.*, vol. 78, pp. 9–11, 2013.
[27] A. S. Chaves, G. G. Rondina, M. J. Piotrowski, P. Tereshchuk, and J. L. Da Silva, 'The role of charge states in the atomic structure of Cu n and Pt n (n= 2–14 atoms) clusters: A DFT investigation', *J. Phys. Chem. A*, vol. 118, no. 45, pp. 10813–10821, 2014.
[28] A. Bendjeddou, T. Abbaz, A. Gouasmia, and D. Villemin, 'Quantum chemical studies on molecular structure and reactivity descriptors of some p-nitrophenyl tetrathiafulvalenes by density functional theory (DFT)', 2016.
[29] A. T. Maynard, M. Huang, W. G. Rice, and D. G. Covell, 'Reactivity of the HIV-1 nucleocapsid protein p7 zinc finger domains from the perspective of density-functional theory', *Proc. Natl. Acad. Sci.*, vol. 95, no. 20, pp. 11578–11583, Sep. 1998.
[30] R. G. Parr, R. A. Donnelly, M. Levy, and W. E. Palke, 'Electronegativity: The density functional viewpoint', *J. Chem. Phys.*, vol. 68, no. 8, pp. 3801–3807, Apr. 1978.
[31] N. Obi-Egbedi, I. Obot, M. El-Khaiary, S. Umoren, and E. Ebenso, 'Computational simulation and statistical analysis on the relationship between corrosion inhibition efficiency and molecular structure of some phenanthroline derivatives on mild steel surface', *Int J Electrochem Sci*, vol. 6, no. 1, pp. 5649–5675, 2011.
[32] D. Laxmi and S. Priyadarshy, 'HyperChem 6.03', *Biotech Softw. Internet Rep. Comput. Softw. J. Sci.*, vol. 3, no. 1, pp. 5–9, 2002.
[33] M. Caricato, M. J. Frisch, J. Hiscocks, and M. J. Frisch, *Gaussian 09: IOps Reference*. Gaussian, 2009.
[34] 'software-index'. Accessed: Jun. 08, 2023. [Online]. Available: https://sites.google.com/view/molecvue/software-index

Chapter 3

Analyzing organic compounds reactivity using DFT

III.1. Introduction

This last chapter is devoted to the correlation of experimental results previously reported in the study of corrosion, in order to better understand the behavior of corrosion inhibitors studied at the molecular scale. First, we present in detail the chosen experimental study, then we describe in detail the DFT and SAR calculation procedure. Finally, an in-depth discussion is conducted on global reactivity parameters, Mulliken charge analysis, as well as SAR indices, in order to clarify the role played by each of the molecules under investigation.

III.2. Experimental background

Corrosion is a significant issue in various industries, such as oil and gas, marine, and automotive, causing extensive damage to metallic structures and leading to financial losses. Plant extracts have gained considerable attention as potential corrosion inhibitors due to their abundance, eco-friendly nature, and low cost.

In recent studies, Nofrizal[1], has extracted epigallocatechin gallate ([(2R,3R)-5,7-dihydroxy-2-(3,4,5-trihydroxyphenyl)-3,4-dihydro-2H-chromen-3-yl]3,4,5-trihydroxybenzoate) (COMP1) from green tea while M.T Saeed and coworkers[2], have obtained chlorogenic acid ((1S,3R,4R,5R)-3-[(E)-3-(3,4-dihydroxyphenyl)prop-2-enoyl]oxy-1,4,5 trihydroxycyclohexane-1-carboxylic acid) (COMP2) from Daucus carota L. peels. The inhibitory role of these previous extracts on mild steel corrosion in acid media was investigated using several laboratory techniques including weight loss test, electrochemical impedance spectroscopy EIS, polarization, and scanning electron microscopy SEM. It was reported that these studied extracts could act as effective corrosion inhibitors. However, the corrosion inhibition efficiency obeys the order: COMP2 > COMP1.

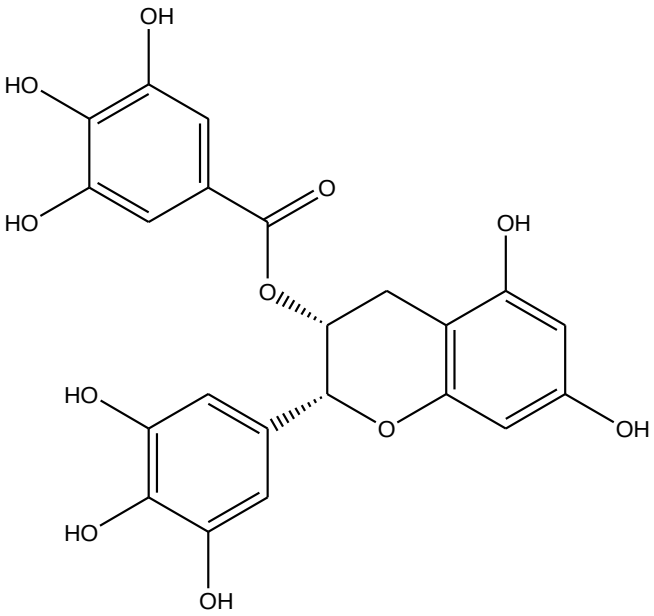

COMP1

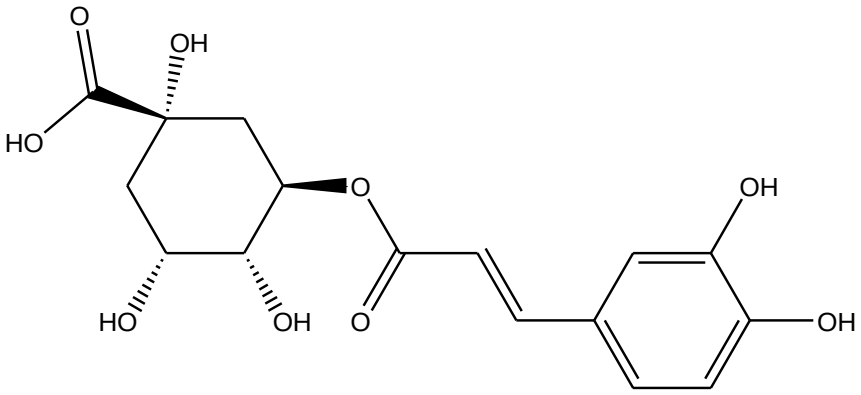

COMP2

Figure III.1: *Optimized molecular tructures of COMP1 and COMP2 corrosion inhibitors*.

To the best of our knowledge, there is no theoretical background has been proposed yet to bridge the gap between the electronic and the molecular properties of the above mentionned corrosion inhibitor candidates and their experimental inhibitory efficacies earlier reported

In this chapter, we attempt to correlate the experimental data of the concerned corrosion inhibitors and their features at the molecular scale. DFT-derived global and local reactivity descriptors, as well as SAR parameters, were calculated and then well discussed to give supportive informations elucidating the experimental findings earlier reported.

III.3. Computational details

The molecular structures of the investigated corrosion inhibitors COMP 1 and COMP 2 were pre-minimized using HyperChem software and then saved as mol files. These lasts were implemented into GaussView 5.0.8 to run the calculations using the Gaussian 09 program package at the Density functional theory level combined with Becke 3 Lee Yang Parr exchange-(B3LYP) correlation hybrid functional with 6-31G basis set. This theoretical level is efficient to give accurate results to be correlated with the experimental observations. To perform the calculation in the aqueous phase, a self-consistent reaction field (SCRF) combined with a polarizable continuum model (PCM) that considers the water molecules as a cavity with a dielectric constant equal to 78.5. DFT outcomes were used to obtain the global reactivity descriptors as mentioned in Chapter 2.The output files were used also to obtain the Mulliken charges of the constitutive atoms of each inhibitor.

Local reactivity was estimated by analysing the Mulliken charges which were calculated at the theoretical level DFT/B3LYP/6-31G to locate the active atoms for electron transfer in the studied molecules.

Structure activity relationship SAR analysis has been performed on the optimized molecular structure at the same theoretical level using HyperChem 8.0 program package. SAR parameters including polarizability (α), partition coefficient (LogP), hydration energy (HE), surface area (SA), and molecular volume (V) are collected and then discussed in detail.

III.4. Results and discussion

III.4.1. Global reactivity outcomes

The behavior of the corrosion inhibitor molecule as a whole can be studied using E_{HOMO}, E_{LUMO}, energy gap(ΔE), hardness(η), softness(S), electronegativity(χ), electrophilicity(ω), and the fraction of electron transferred from the inhibitor to the metal surface(ΔN), collectively named global reactivity descriptors. The optimized molecular structures of the corrosion inhibitors under probe as well as their related global reactivity parameters, calculated at the

DFT/B3LYP/6-31G level of theory, are exhibited in Figure III.2 and Table III.1, respectively.

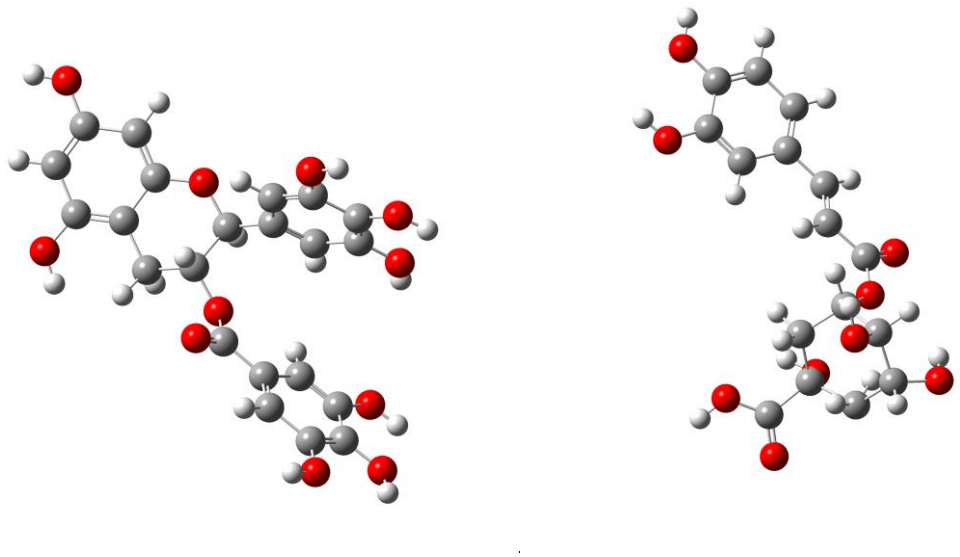

Figure III.2: *Optimized molecular structures of COMP1 (a) and COMP2 (b) corrosion inhibitors, calculated at DFT/B3LYP/6-31G level of theory.*

Table III.1: *The obtained global reactivity descriptors of the studied corrosion inhibitors, calculated in the aqueous phase at DFT/B3LYP/6-31G level of theory.*

Quantum parameter	COMP1	COMP2
E_{HOMO} (eV)	-6.039	-6.069
E_{LUMO} (eV)	-1.606	-2.137
ΔE (eV)	4.433	3.931
I (eV)	6.039	6.069
A (eV)	1.606	2.137
Ƞ (eV)	2.216	1.966
S (eV^{-1})	0.451	0.509
ω	3.296	4.282
χ (eV)	3.822	4.103
μ Debye	8.766	14.037
ΔN	3.521	2.847

According to the frontier molecular orbital theory proposed by Fukui Kinachi, Both the highest occupied molecular orbital (HOMO) and lowest unoccupied molecular orbital (LUMO) are responsible for the chemical reactivity. HOMO is the orbital having the tendency can donate electrons, its donation power increases with the increase of its energy E_{HOMO}[3]. Conversely, LUMO is the orbital that could accept electrons its acceptance capacity to receive electrons increases with a decrease in E_{LUMO}[4]. The electronic distribution of HOMO and LUMO frontier orbitals across the investigated molecular systems is depicted in Figure III.3. As can be seen from Table III.1, the inhibitor COMP1 has E_{HOMO} less than that of COMP2, this theoretical result validate the order of inhibition effectiveness earlier reported. Besides, E_{LUMO} values decrease following the sequence: COMP1 > COMP2, which correlates with the experimental observations.

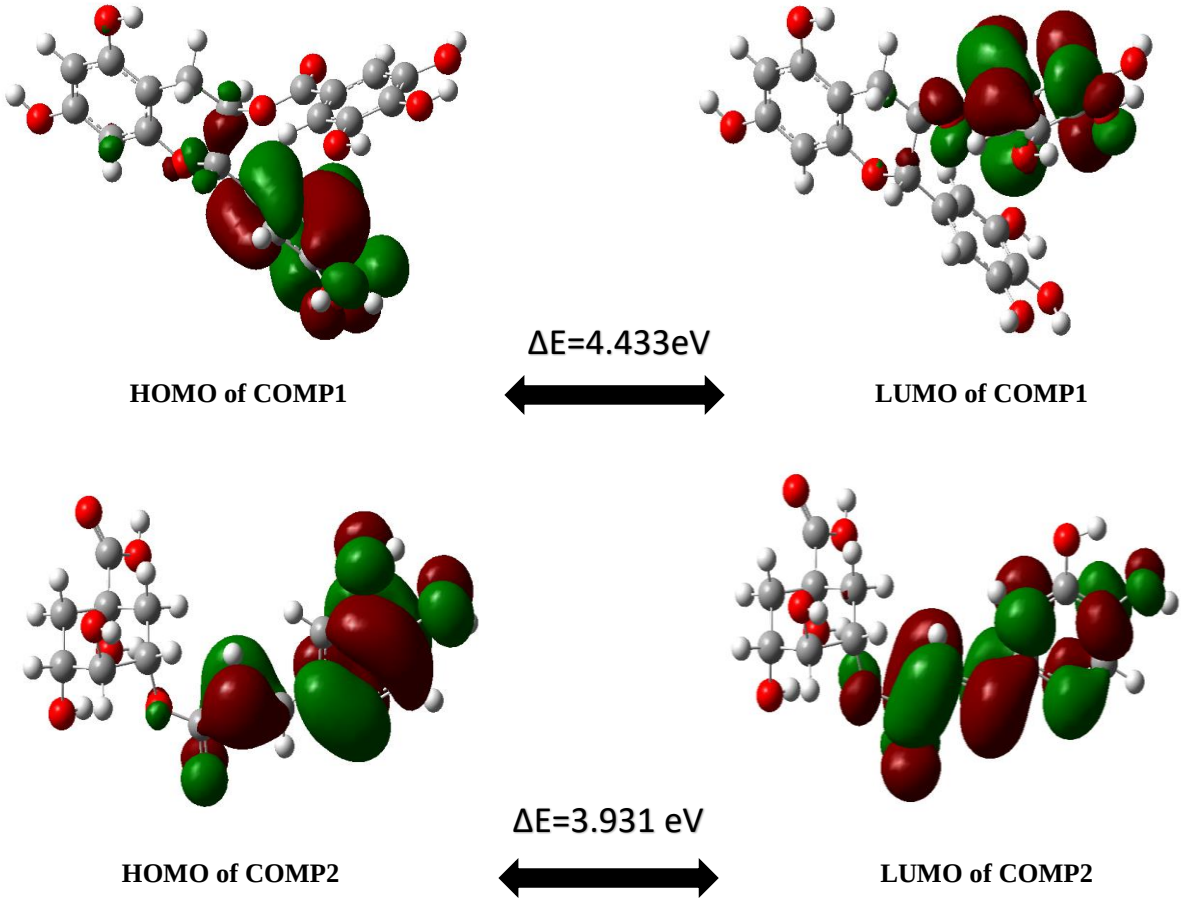

Figure III.3 : *HOMO-LUMO electronic distribution in the studied molecular structures.*

The energy gap (ΔE); LUMO-HOMO energy difference is also important quantum parameter used to assess the reactivity of the corrosion inhibitor compounds. The molecule with

the least energy gap is predicted to be an excellent corrosion inhibitor[5]. According to results displayed in Table III.1, the ΔE increases as follows: COMP1 > COMP2, suggesting that COMP2 can protect the targeted mild steel against aggressive agency more than COMP1, this result is in full agreement with experimental findings.

The chemical hardness(η) and its reciprocal(S) are two crucial quantum indices extremely used to assess the reactivity of different chemical species. The chemical hardness measures the molecule's resistance to the electron cloud perpetration during the reaction. Molecules having lower hardness values have the tendency to easily adsorb into the mild steel substrate leading to higher corrosion protection[6]. It can be seen from Table 1 that the chemical hardness values follow the trend: COM1 > COMP2 which means that the softness values follow the trend: COMP2 > COMP1, These results emphasize the order of the inhibition efficiency earlier reported.

Electronegativity(χ)[7], represents the aptitude of a molecule to attract an electron from its surrounding chemical environment. This quantum parameter is a key factor in corrosion science; the chemical compounds with lower electronegativity are expected to be satisfied corrosion inhibitorsThe electronegativity data given in Table III.1 reveal that COMP2 has greater electrosensitivity than COMP1, this result is in contradiction with the experimental outcomes.The dipole moment(μ)is a beneficial descriptor[8], that informs about the polarity of the chemical species, a polar molecule should have a dipole moment different than zero. The dipole moment can be used to assess the reactivity of a corrosion inhibitor candidate toward the metal surface, the molecules possessing a high dipole moment could serve as excellent inhibitors to prohibit the metal against corrosion. table III.1 shows that the tendency of the electronegativity of the tested inhibitors is: COMP2 > COMP1, which does not agree with the experimental results previously noticed.

The electron transfer from the inhibitor to the poor metal surface (ΔN) can be quantified using the Pearson formula as described in Chapter II. According to Lukovits et al[9], the inhibitor candidate could give electrons to the deficient metal surface if (ΔN) is positive and less than 3.6. The electron donation ability with the increase of ΔN. The data of ΔN displayed in Table III.1 declares that the studied corrosion inhibitors are electron donors to the vacant d orbital of the metal, the donation order is as follows: COMP2 < COMP1, which does not confirm the trend of the inhibitor efficiency.

Electrophilicity is a quantum index that determines the capacity of a molecule to accept an electron. Molecules having lower electrophilicity are predicted to prevent the metal surface corrosion, as observed from table1the trend in electrophilicity is as follows: COMP2 > COMP1.

III.4.2. Mulliken charge analysis

Mulliken charge analysis is a method used to calculate the partial charges on atoms in a molecule. By analyzing these charges, we can identify regions of positive or negative charge, which can help us determine the electrophilic and nucleophilic sites.

The electrophilic sites are the molecular regions with partially positive charges or positive Mulliken charges that are often considered electrophilic. These regions are electron-deficient and tend to attract nucleophiles. Nucleophilic sites represent the regions with partially negative charges or negative Mulliken charges that are typically considered nucleophilic. These regions are electron-rich and have a higher electron density, making them more likely to donate electrons. Common nucleophilic sites include lone pairs on atoms like oxygen, nitrogen, and sulfur, as well as negatively charged ions.

The Mulliken charge distribution across a molecule can be used to predict the eventual central adsorption. For corrosion inhibitors, the greater the negative charge, the greater its ability to donate electrons. The most negatively charged regions are the most likely adsorption centers. The Mulliken charges of the constitutive atoms and their numbering for each corrosion inhibitor are listed in Table III.2 and Figure III.4, respectively.

Table III.2: *the Mulliken atomic charges of comp1 and comp2.*

COMP1		**COMP2**	
Atoms	**Mulliken charge**	**Atoms**	**Mulliken charge**
C1	0.1917	C1	0.1567
C2	0.2756	C2	0.1070
C3	0.0302	C3	0.2690
C4	0.1335	C4	0.2518
C5	0.2299	C5	0.2649
O6	-0.5905	C6	0.0916
C7	0.0117	C7	0.5303
C8	0.2478	O8	-0.4357
C9	0.0235	**O9**	**-0.1504**

C10	0.1675	O10	-0.2631
O11	-0.2442	O11	-0.2431
O12	-0.2565	**O12**	**-0.2339**
C13	0.4802	O13	-0.5498
C14	0.0105	C14	0.4975
C15	0.0628	C15	0.0127
C16	0.2579	C16	0.0262
C17	0.2532	O17	-0.4904
C18	0.2529	C18	0.0712
C19	0.0618	C19	0.0253
O20	-0.4675	C20	0.2531
O21	-0.5401	C21	0.2613
O22	-0.2470	C22	0.0420
O23	**-0.2262**	**C23**	**-0.0192**
O24	**-0.2396**	O24	-0.2372
C25	0.0759	O25	-0.2379
C26	0.0245	-	-
C27	0.2551	-	-
C28	0.2362	-	-
C29	0.2525	-	-
C30	0.0197	-	-
O31	-0.2538	-	-
O32	**-0.2430**	-	-
O33	-0.2464	-	-

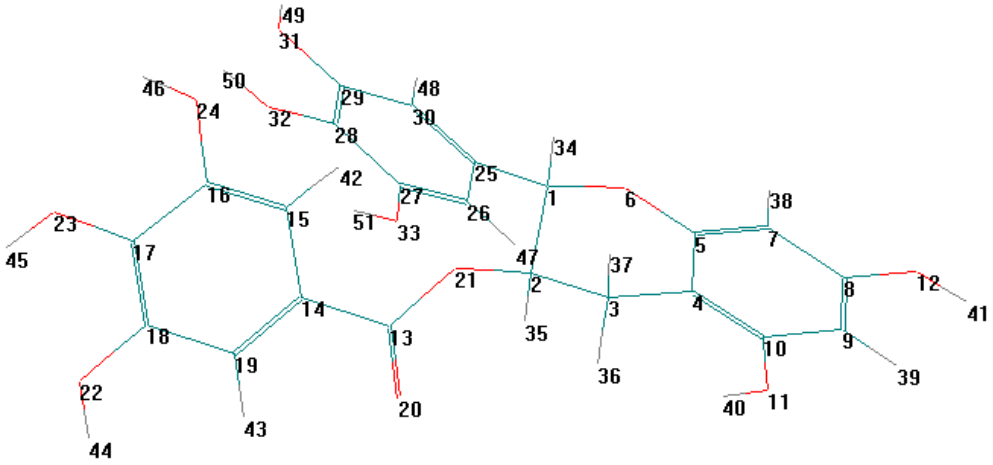

COMP1

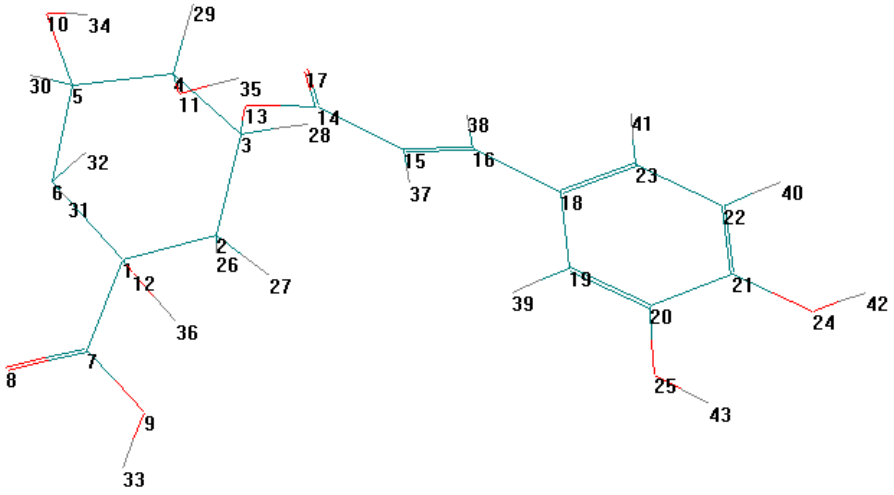

COMP2

Figure III.4*: Atomic numbring for the studied inhibitors.*

For COMP1, the most favorable sites for the nucleophilic attack occurring between the inhibitor and the metal surface are the atoms: O23 and O24, and O32 which have the highest negative charges. For COMP2, the O23 and C9, and O12 atoms possess the highest negative charges compared to the other atoms which indicate that these centers have the greatest tendency to participate in the nucleophilic attack with the electron-deficient metal.

III.4.3. SAR results

SAR calculations have been applied and several parameters have been obtained and resumed in Table III.3. The polarizability (α) measures the change in the electronic distribution of the molecule with respect to the applied electric field. When the polarization increases, the intrinsic molecular value increasing the adsorption of the molecule to the metal surface becomes easier leading to high inhibition efficiency[10]. According to the results of Table III.3, the polarizability obeys the following order: COMP2 < COMP1,which indicates a negative correlation with the inhibition efficacies previously reported.The partition coefficient (LogP) is an important parameter to assess the anticorrosive activity of a molecule[11]. As (LogP) increases, the water solubility of the molecule decreases. Therefore, the electronic transport to the metal surface becomes slower and the adsorption will be weak. As shown in Table III.3, (LogP) increases as follows: COMP1 < COMP2, which is in a bad relationship with the experimental results.

The hydration energy (HE) of molecules measures the degree of dissolution. Negative values of the hydration energy of the molecule being studied indicate exothermal dissolution. The increase in the hydration energy leads to an increase in the efficiency of the molecule [11].Regarding the data listed in Table 3, the hydration energy (HE) decreases following the sequence: COMP2 > COMP1, this result fully agrees with the trend of the inhibition efficiency.

The molecular volume illustrates the possible coverage of a metallic surface by the inhibitor. The compound having a large molecular volume value has the highest surface coverage and therefore could give high protection performance to the metal surface. The efficiency of inhibition accelerates when the molecular volume increases due to the improvement of the contact gap between the molecule and the surface. A comparison of molecular volume values across the studied structures highlights the order: COMP1 > COMP2. Therefore, the order of inhibition efficacy would preferentially be COMP1 > COMP2, which is not consistent with the order of inhibition efficacy of the compounds.

Table III.3: *SAR parameters of the corrosion inhibitors under investigation.*

SAR parameters	COMP1	COMP2
α (A^3)	42.78	32.45
V (A^3)	1123.36	934.83

SA (A^2)	642.23	560.36
HE (kcal/mol)	-50.52	-31.75
LogP	-5.94	-2.22

References

[1] N. Nofrizal, 'Corrosion Inhibition Of Mild Steel In 1m HCL By Catechin Monomers From Commercial Green Tea Extracts', *Sci. Contrib. Oil Gas*, vol. 35, no. 1, pp. 11–24, Feb. 2022, doi: 10.29017/SCOG.35.1.773.

[2] M. T. Saeed, M. Saleem, A. H. Niyazi, F. A. Al-Shamrani, N. A. Jazzar, and M. Ali, 'Carrot (Daucus carota L.) peels extract as an herbal corrosion inhibitor for mild steel in 1M HCl solution', *Mod. Appl. Sci.*, vol. 14, no. 2, pp. 97–112, 2020.

[3] I. A. Adejoro, D. C. Akintayo, and C. U. Ibeji, 'The efficiency of chloroquine as corrosion inhibitor for aluminium in 1M HCl solution: Experimental and DFT study', *Jordan J. Chem.*, vol. 11, no. 1, pp. 38–49, 2016.

[4] H. Ashassi-Sorkhabi, B. Shaabani, and D. Seifzadeh, 'Corrosion inhibition of mild steel by some Schiff base compounds in hydrochloric acid', *Appl. Surf. Sci.*, vol. 239, no. 2, pp. 154–164, 2005.

[5] Y. Yan, W. Li, L. Cai, and B. Hou, 'Electrochemical and quantum chemical study of purines as corrosion inhibitors for mild steel in 1 M HCl solution', *Electrochimica Acta*, vol. 53, no. 20, pp. 5953–5960, 2008.

[6] N. Obi-Egbedi, I. Obot, M. El-Khaiary, S. Umoren, and E. Ebenso, 'Computational simulation and statistical analysis on the relationship between corrosion inhibition efficiency and molecular structure of some phenanthroline derivatives on mild steel surface', *Int J Electrochem Sci*, vol. 6, no. 1, pp. 5649–5675, 2011.

[7] J. Saranya, P. Sounthari, K. Parameswari, and S. Chitra, 'Adsorption and density functional theory on corrosion of mild steel by a quinoxaline derivative', *Pharma Chem.*, vol. 7, no. 8, pp. 187–196, 2015.

[8] N. Khalil, 'Quantum chemical approach of corrosion inhibition', *Electrochimica Acta*, vol. 48, no. 18, pp. 2635–2640, 2003.

[9] I. Lukovits, E. Kalman, and F. Zucchi, 'Corrosion inhibitors—correlation between electronic structure and efficiency', *Corrosion*, vol. 57, no. 1, pp. 3–8, 2001.

[10] H. Rahal, A. Abdel-Gaber, and G. Younes, 'Inhibition of steel corrosion in nitric acid by sulfur containing compounds', *Chem. Eng. Commun.*, vol. 203, no. 4, pp. 435–445, 2016.

[11] O. A. El-Shamy, 'Semiempirical theoretical studies of 1, 3-benzodioxole derivatives as corrosion inhibitors', *Int. J. Corros.*, vol. 2017, 2017.

General conclusion

General Conclusion

In this scientific contribution, SAR and DFT calculations have been performed in the aqueous phase at DFT/B3LYP/6-31G theoretical level to explain the relationship between the order of the studied corrosion inhibitors and their electronic features at the molecular scale. In the light of the previous discussions, we can conclude:

- Global reactivity descriptors including dipole moment, energy gap, hardness, and softness, correlate experimental inhibition effectiveness.
- SAR parameters including surface area, hydration energy, and volume validate the order of inhibition efficiency reported experimentally whereas the Log P partition coefficient does not validate this order.
- The Mulliken charge analysis for both inhibitors under probe gives a reactive scheme localizing the reactive atomic sites responsible for the nucleophilic attack between the inhibitor molecule and the vacant d orbital of the targeted metal.